SELF-FOLDING MICROGRIPPERS AND THEIR APPLICATIONS AS BIOMEM SYSTEMS

by
Beril Polat

A thesis submitted to Johns Hopkins University in conformity with the requirements for the degree of Master of Science in Engineering in: Chemical and Biomolecular Engineering.

Baltimore, Maryland
May 2016

Abstract

Self-actuating microtools have evolved to be more efficient as diagnostic biological microelectromechanical (bioMEM) systems because of their miniature and robust designs. One of these microtool designs, namely microgrippers, is fabricated and used with the purpose of single cancer cell and tumor lesion diagnostics. They are self-actuated tools that can be used tethered or untethered with many potential applications in the field of medicine.

Self-folding microgrippers have different applications depending to their dimensions and designs. We utilized single cell microgrippers as micro-arrayed diagnosis tools by capturing mammalian cells in vitro without causing any damage. Since the microgripper design allows for nutrients in the environment to diffuse in and out of the cell between the gripper arms, the cells stay viable over 24 hours, which facilitates dynamic observations on the cells. We successfully detected specific molecules in a captured cell using surface-enhanced Raman spectroscopy (SERS). Additionally, thermally-responsive untethered grippers can be used as soft tissue sampling tools with high resolution compared to conventional biopsy forceps. The addition of a thin nickel film on the gripper arms provides better motion control in vivo and thus, better coverage of the sampling area. Although the efficiency of these grippers was proven in a statistical model, we designed an in vivo statistical sampling study to support this model. Finally, we implemented a biocompatible actuation mechanism, capable of keeping the gripper arms open until reaching a tissue wall.

Potential applications of microgrippers are extensive. Depending on their dimension, design, and the fabrication materials used, it is possible to adapt them into any

desired application. Therefore, they are one of the pioneer designs in microtool systems in medicine. In this thesis, I aim to give a review of different microgripper designs from other research teams and explain our design and its applications.

Advisor/PI: David H. Gracias, Ph.D.

Second reader: An Goffin, Ph.D.

Acknowledgements

Foremost, I would like to express my gratitude to my supervisor Professor David Gracias for the useful comments, advice and commitment through the learning process of this master thesis. I would also like to acknowledge Dr. An Goffin for accepting to be the second reader to my thesis and her support and time throughout my undergraduate and graduate years at Johns Hopkins University. Additionally, I would like to thank Kate Malachowski for taking me on board to her PhD project, which introduced me to this topic as well as her constant support inside and outside the lab. She brought out the scientist in me who was eager to learn new information. I also cannot forget to thank my brilliant lab partner, Qianru Jin for guiding me and working with me throughout my research presented in this thesis and for all the useful lab techniques I have learned from her.

I like to thank to my fellow lab mates, Arijit Ghosh, Hye Rin Kwag, ChangKyu Yoon, and Jayson Padaguan, who willingly shared their time and knowledge during the times in lab. In addition, I would like to acknowledge the support from all my friends outside the lab for making me feel like I wasn't just a scientist or engineer.

Last but not the least, my sincere thanks goes to my loved ones, my mom, my dad and my brothers for their unconditional love and support throughout my life. If my parents didn't believe in me and send me to the United States for college, I wouldn't be here in the first place. Also, I would like to thank Evan Johnson for making me feel motivated and loved throughout college and graduate school. If it wasn't for them, I wouldn't be able to successfully balance school and social life.

To my family and my grandmother, Aynur Suna

Table of Contents

List of Figures

Chapter 1: Minimally invasive microsurgery tools: microgrippers

1.1 Existing technology and its applications

We are in an age of technology that continuously seeks to find minimally invasive tools for biology and biomedical applications. As the designs of these tools improve, the need for miniaturization and better resolution becomes more apparent. There are many microtools in progress in the field of bioMEMs that aim to be eventually used in medicine, specifically for diagnosis of a precancerous lesion and surgical operations. One of these microtool designs, called microgrippers, has the purpose of micro and nano manipulation of biological organisms, which range in size from 1 μm to 1 mm.[1] However, scaling down to the micron or even nano-scale comes with physical limitations and problems.

In order for microgrippers to be used as commonly as large size medical tools, they must have high precision, be easily manipulated and affordable. In addition to these properties, the design of these tools must include the necessary means of maneuverability, actuation, retrieval, and signal sensing with minimal damage to the specimen.[2] Therefore, since the 1900s there has been a great amount of research to improve these issues, and they will be addressed in this thesis.

Beginning in 1991, Kim et al. designed surface micromachined polysilicon microgrippers that are electrostatically actuated to perform a gripping function.[3,4] They were able to grab an euglena, a one-cell protozoa, but their grippers couldn't function in a liquid environment so the euglena was deceased. Although these electrostatic actuators offered the highest frequency with lowest power consumption of all grippers discussed in this section, the microgripper shapes were complicated to fabricate and required a high

operation voltage.[5] In addition, Kim et al. observed stickiness between the gripper jaws and the test specimen which caused difficulty in releasing the specimen [FIGURE 1].

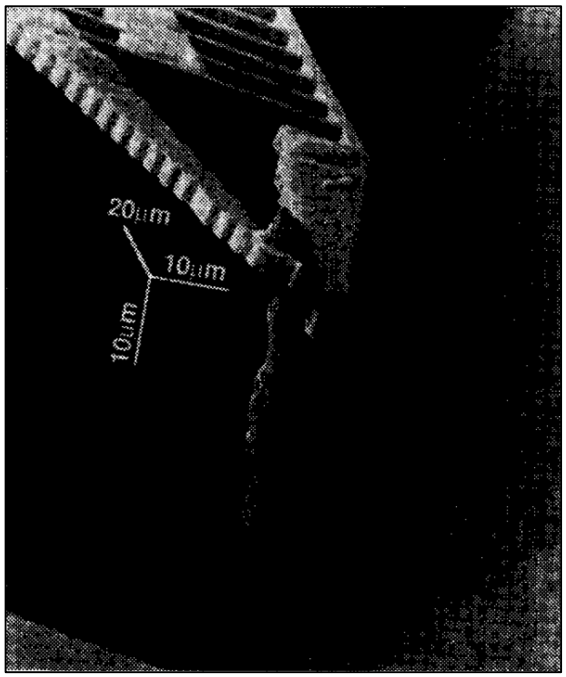

Figure 1: SEM picture of a protozoa, a euglena, being held by the microgripper. The euglena is 40 μm long and 7 μm in diameter. (Copyright © 1992, IEEE)

In 1992, Pister et al. proposed a similar microgripper design with a new surface micromachining process.[6] They fabricated a parallel-plate gripper with a hinge technology, which offered fabrication of microgrippers at a scale that was difficult to obtain with the previous micromachining techniques. The actuation was done mechanically with the release of handles. This made it possible to convert the actuators that were separate from the chip to an on-chip mechanism during the fabrication. Pister et al. improved the micromachining process but the problems of small gripping force and low structural rigidity persisted. In an effort to reduce these problems, Lee et al. developed a microgripper that can be actuated at lower temperatures (<100°C), has a

larger gripping force (>1mN) and has higher structural rigidity.[7] They achieved these results by designing a nickel-titanium-copper shape memory film that goes through a crystalline phase transformation due to tensile residual stress [FIGURE 2]. The $Ni_{42}Ti_{50}Cu_8$ alloy transformed just above body temperature, 37°C, and was fully actuated at 70°C.

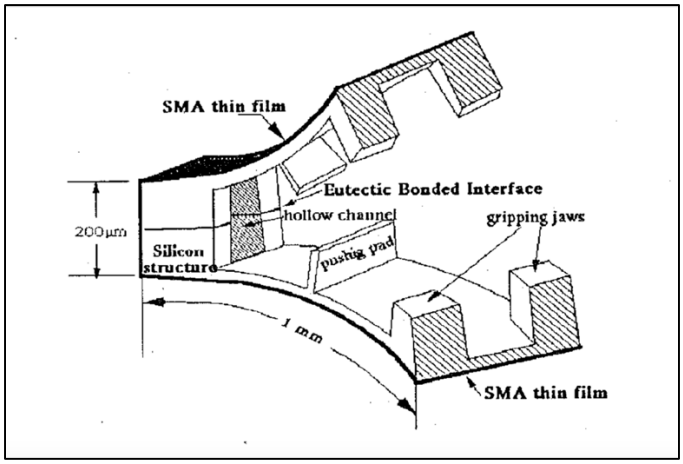

Figure 2: Three dimensional schematic of microgripper (Copyright © 1996 Published by Elsevier B.V.)

At the beginning of the 2000s, the microgripper designs started to acquire different purposes such as changing the operating environment and increasing the motion of the gripping arms. By designing a microrobotic arm composed of a conjugated polymer bilayer, Jager et al. achieved a system that can operate in a liquid environment.[8] The arms of the microrobots consisted of an elbow, a wrist, and a hand with jointed fingers, closely resembling a human arm. The flexible joints were made up of polypyrrole (PPy)/Au bilayer and acted as the microactuators when the team applied a cyclic voltammetry on the bilayers [FIGURE 3]. The actuation was due to the oxidation and reduction of the PPy layer caused by the positive or negative potential applied on the Au

layer. They proved the feasibility of this design by grabbing and lifting a 100 μm glass bead and claimed that the robot arms could be used in salt solutions, blood plasma, urine and cell culture medium.

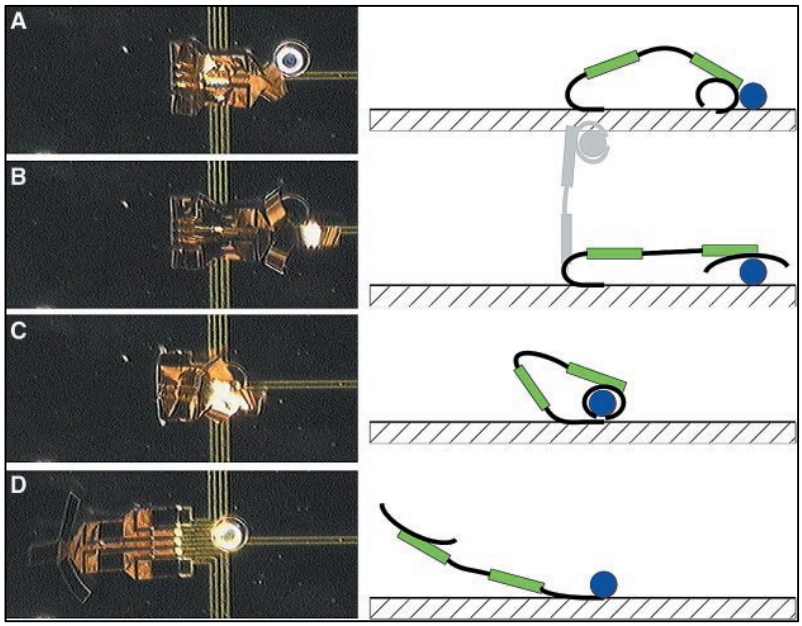

Figure 3: (A through D) A sequence of pictures (left) showing the grabbing and lifting of a 100-mm glass bead and schematic drawings of the motion (right). In this case, the arm has three fingers, placed at 120° from each other. (Copyright © 2000, The American Association for the Advancement of Science)

In 2002, Volland et al. tried to upgrade the linear motion of the microactuators to a rotational gripping motion using a system of elastic spring beams.[9] They were also able to decrease the fabrication steps to make the microgrippers more affordable and more reliable. However, their grippers required high operating voltage of 80-90 V [FIGURE 4]. In 2006, the applications of these microgrippers expanded to biological systems. Wierzbicki et al. utilized the electrostatically driven microgrippers to measure the contraction forces on the blood vessel walls.[10] They fabricated the grippers using silicon micromachining technology and anticipated future applications in aorta vessels.

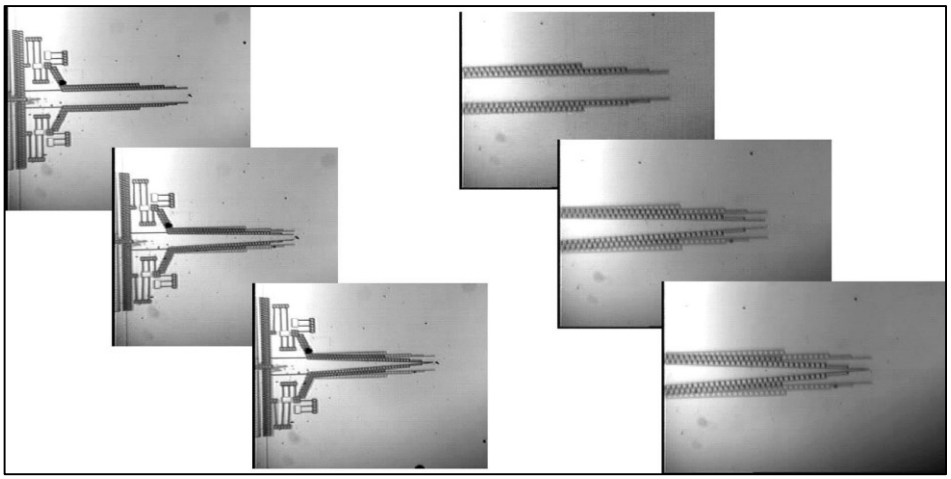

Figure 4: Operation of the microgripper using a system of elastic spring beams (Copyright © 2002 Elsevier Science B.V. All rights reserved.)

In the same year, Luo et al. modelled and fabricated "normally-closed" microgripper structures, which they called microcages, consisting of a polymer (SU-8)/ metal (Aluminum)/ diamond like carbon (DLC) trilayer structure.[11] The group took advantage of the differences in the thermal expansion coefficients of SU-8 and DLC and used Al as the heating electrode in between them. Since the SU-8 layer expanded more than the DLC layer as the temperature increased, it formed a compressive thermal stress on the top of the layer which led to the opening of the arms [FIGURE 5]. Their work was superior to other previously reported microgripper devices because they only had to apply 3.2 V to open the gripper, and without any voltage, it stayed closed.

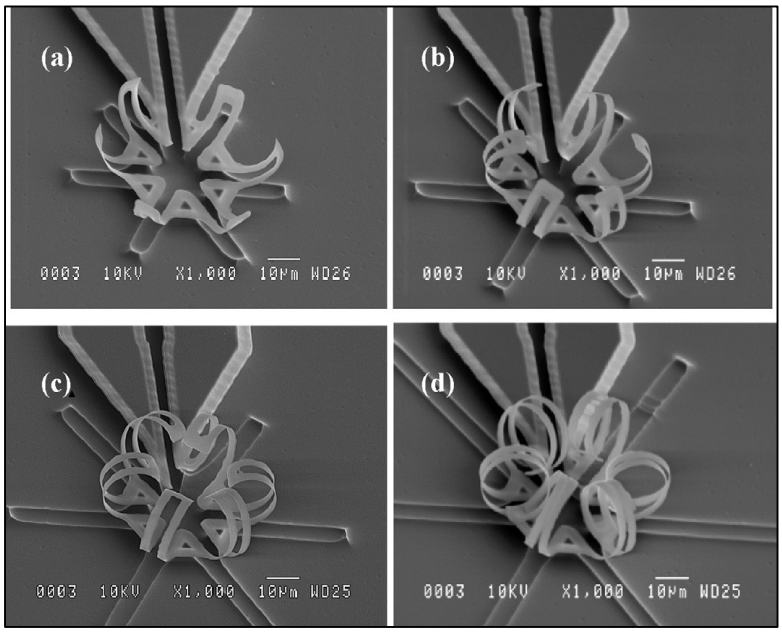

Figure 5: SEM images of SU8/DLC microcages with L of (a) 20 μm, (b) 30 μm, (c) 40 μm, and (d) 50 μm (Copyright © 2006 Elsevier B.V. All rights reserved.)

A similar design with a different actuation mechanism was proposed by Lu and Kim. They proposed a microhand with four fingers that had multiple phalanges connected by joints (i.e., balloons) and as a whole it resembled an arm with muscles that could get actuated pneumatically.[12] Applying pressure inflated the balloon joints which in return flexed the fingers and closed the hand. When they were deflated, the fingers extended and opened the hand [FIGURE 6]. They were able to grab and detach submillimeter biological samples but they were not able to move them around. In addition, this design could operate in aqueous solutions such as salt solutions, silicon oil, and cell culture medium which achieved the goal for moving in to biological environments.

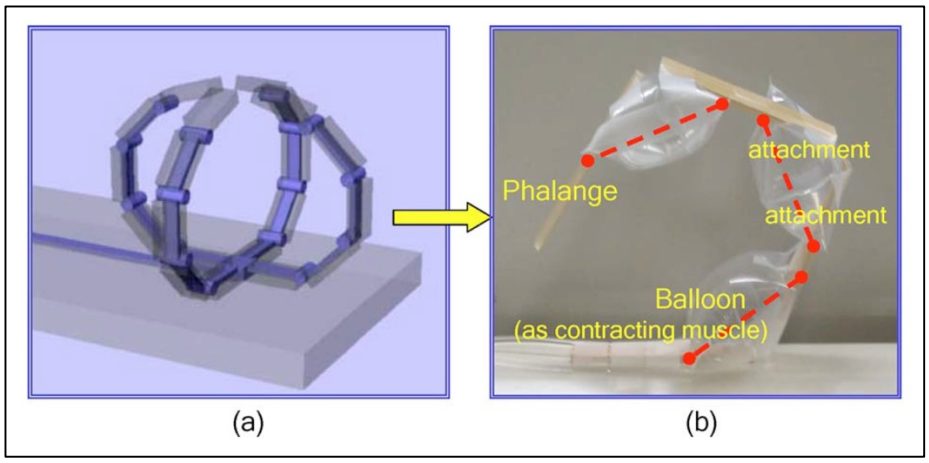

Figure 6: (a) Schematic drawing of a microhand device with four fingers. (b) The actuation mechanism is illustrated in a simplified centimeter-scale experiment. (Reprinted from "Microhand for biological applications" with the permission of AIP Publishing.)

Taking the design one step further, Beyeler et al. monolithically fabricated microgrippers with a force sensor and a feedback system.[13] They envisioned that in order for grippers to be useful in biomedical applications, they had to have good control over the movements with force feedback so that living organisms would not be damaged during the manipulation. Their microgrippers could handle objects within the size range of 5 to 200 µm, be actuated electrostatically, provide real-time force feedback of the gripping force and be used in aqueous environments for cell manipulation. The fabrication was a silicone-on-insulator (SOI) process like the previous electrostatically actuated microgrippers, but had an additional force feedback sensor on it. Thus, the uniqueness of this design came from its sensitivity to the manipulation force. With these grippers, Beyeler et al. were able to perform pick-and-place manipulation of glass spheres in a size range of 20 to 90 µm in diameter and of HeLa cells with an approximate diameter of 20 µm [FIGURE 7].

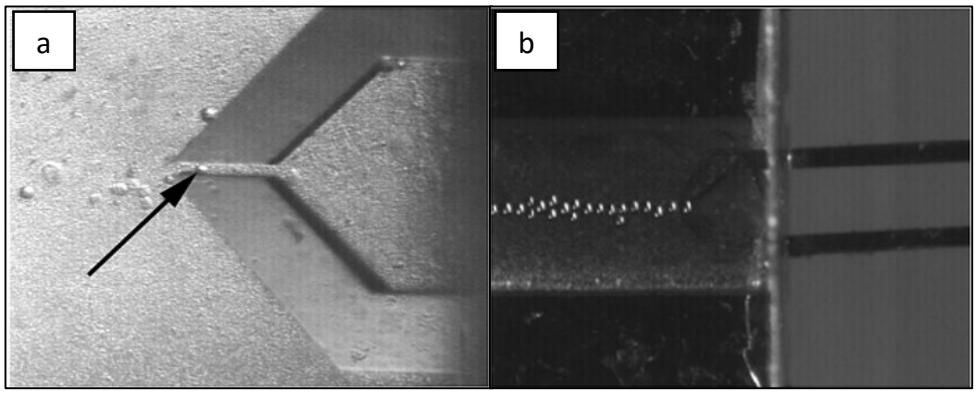

Figure 7: Pick-and-place manipulation of a) a HeLa cell b) a glass sphere (Copyright © 2007, IEEE)

Since 1991, materials such as silicon, steel, nickel and polymers were used for fabrication of microgrippers.[14,15,16,17] In addition to these materials, SU-8, an epoxy-based negative photoresist, is also a commonly used biocompatible material for biological and cell operations. Hence, there have been different designs of microgrippers using SU-8 as their main material for fabrication.[17,18,19,20] One of the latest designs with SU-8 was from Zhang et al.[21] They used three parts for their grippers: a chevron electrothermal actuator, a compliant amplification mechanism and jaws. The actuator was a three layer (Cu-SU8-Cu) structure and only required 90-195 mV voltage to open and close the arms with a response time of 0.23 s. This voltage was smaller than previous gripper designs. After fabrication and characterization, they tested the microgrippers by micro-manipulating a micro blood vessel (with a diameter of 80 μm) and a cyanobacteria cell (with a diameter of 9 μm). The motion of the cell was two dimensional (vertically and horizontally).

As of now, there are many microgripper designs with different materials and actuator systems. However, most of these actuator systems require electrical or mechanical input and this type of actuation could only work with a complicated fabrication system (external wires, sensors, electrical connections, etc) which limits the

maneuverability. In order for these microgrippers to move into medical applications and not just function as an in vitro tool, it is essential that they have an untethered design with high maneuverability and are biocompatible.

1.2 Challenges

The challenges in conventional microgrippers come from the fact that their maneuverability is restricted by the wires/connections between the controller for the actuation mechanism and the gripper jaws/arms. Considering that they always have to be tethered to the controller, their freedom of movement is only two dimensional during the capture of biological samples. In fact, previous designs could only pick-and-place the objects in a 2-D plane rather than 3-D movement. Additionally, the tethered design makes it challenging to reach through a sub-millimeter size tube (such as intestines, esophagus, blood vessel, etc.) for retrieval of any samples (tumor lesion, damaged tissue, single cell, etc.). Therefore, former microgripper designs are limited to work in vitro only.

Another challenge emerges in the actuation method of the gripper arms/jaws. Electrical, mechanical and pneumatic actuations can give better control over the gripper movement on a 2-D plane because of the feedback system that is built within the controller. However, these actuations are hard to achieve and maintain in an aqueous or biological environment. Hence, it is more practical to have an actuation based on chemical or thermal cues. For example, actuation based on pH, salt concentration, enzymatic activity, or temperature can be used in an in vivo or ex vivo setting because these parameters vary between very specific concentrations and numbers and are crucial for the survival of single cells and cell colonies.

Previously in our lab, Leong et al. proposed a design for microgrippers that have both high maneuverability and a bio-friendly actuation mechanism.[22] They designed microgrippers that resemble a human hand with palm and fingers (called "rigid panels" or "phalanges") with joints. The microgrippers were 700 μm when open (tip-to-tip) and 190 μm when closed. The joints between the fingers were composed of a trilayer film (a polymer and two metallic thin films) and due to the differences in the residual tensile stress in the metal layers, they could bend in one direction. After experimental testing, they were able to determine that the release of residual stress in a 50 nm Cr coupled with a 200-250 nm Cu thin film resulted in a 90° bending on the gripper arms. The actuation for bending was controlled by the third polymer layer. This layer was a cresol novolak resin (a commercial photoresist) which behaved like a neutralizer for the competitive bending force between the two metal layers. At room temperature or below, this resin preserved its hardness, preventing the bending of the metal films and keeping the arms open. When heated, the resin got soft enough to let bending occur and thus closing of the arms [FIGURE 8]. Additionally, they fabricated the phalanges with Ni (ferromagnetic metal) so that the grippers could be precisely controlled and moved around which increased the maneuverability even more.

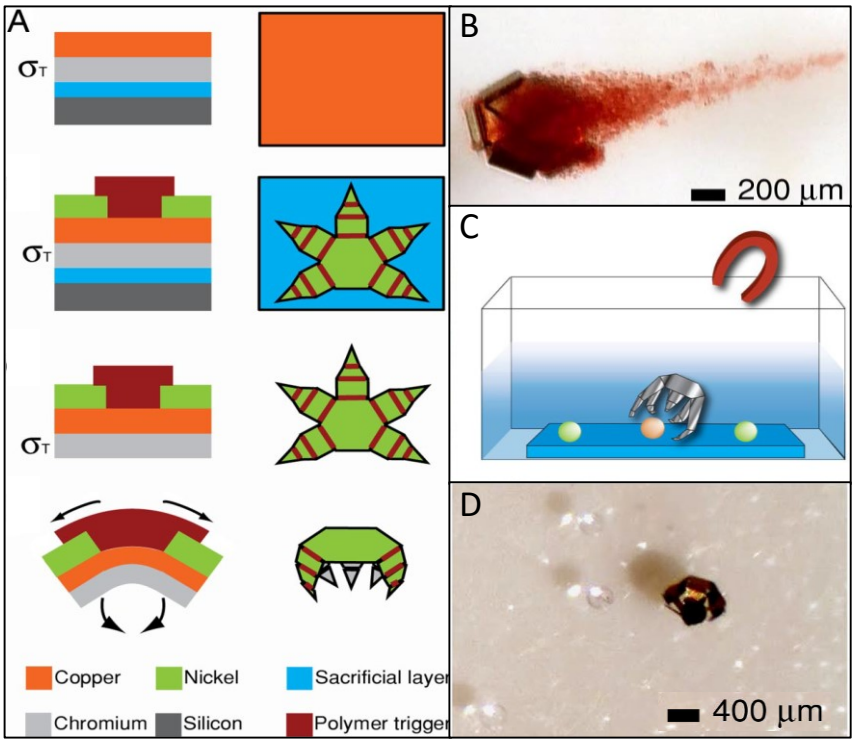

Figure 8: a) Schematic of the fabrication and operation b) Microgripper with the captured tissue c) Schematic depicting magnetically directed movement and capture of a bead d) Thermally triggered capture of a dyed bead (275 µm) (Copyright © 2009 by the NAS)

Given the advantages of this new tetherless design of microgrippers, it was possible to retrieve biological samples in aqueous environment and in elongated coiled tubes. In 2010, a year later, Bassik et al. from our lab improved the design of these metallic tetherless grippers by triggering the closing of the arms enzymatically.[23] They used the difference in residual tensile stress between Cr and Au thin films with Ni layer incorporated to bend the arms and tested two different biopolymer actuation layers. These polymers were gelatin, which gets degraded by proteases, and carboxymethylcellulose (CMC), which gets degraded by glucosidases. Having both of these biopolymers that are degraded by different enzymes gave grippers the capability of reopening after a closure. This was the proof that it is possible to design tetherless microgrippers with self-actuation

and folding mechanisms. In addition, the specificity for certain cell types could be enhanced by altering the enzyme-substrate interaction in the trigger layer.

By overcoming the two main challenges (maneuverability and bio-friendly actuation) in microgripper design, Leong and Bassik et al. started a chain of great improvements. For example, Gultepe et al. used these tetherless and thermally-responsive microgrippers (tip-to-tip size varying from 300 μm to 1.5 mm) to perform ex vivo and in vivo biopsies on a bile duct from a porcine liver and a bile duct from a live pig respectively.[24,25] They used magnets to control the movement of the grippers inside the bile duct. Although these biopsies with the microgrippers were successful, the smallest size of tissue sample that these grippers could retrieve was around 0.25 mm^2 and the fabrication with the polymer trigger layer needed some optimization. Therefore, my goals for the next step included proving the resolution advantage of the tissue microgrippers in an esophagus over conventional forceps and designing microgrippers on a single cell level in order to have single cell analysis of the diseased lesions.

Chapter 2: Self-folding single cell microgrippers

The main challenge in tumor detection is caused by the tumor heterogeneity. This is the observation that different tumor cells can show distinct morphological and phenotypic profiles, including cellular morphology, gene expression, metabolism, motility, proliferation, and metastatic potential.[26] Due to the heterogeneous nature of cultures, tumors, and tissues, the ability to capture, contain, and analyze single cells has become essential for genomics, proteomics, diagnostics, therapeutics and surgery. Unfortunately, the current approaches to tumor detection mask cellular heterogeneity and dynamics and are limited to rare and heterogeneous cell populations, such as stem cells.[27,28] They tend to look at the average of assays, which may not accurately represent the behavior of the individual cells, particularly if the cells of interest are a small fraction of the population, such as stem cells, immune cells, and cancer cells.

There are existing methods to overcome heterogeneity to analyze single cells such as fluorescence-activated cell sorting (FACS)[29], droplet-based microfluidics[30], microwells or nanopillars[31], and laser capture microdissection[32]. FACS provides a method for sorting a heterogeneous mixture of biological cells based upon the specific light scattering and fluorescent characteristics of each cell. Droplet-based microfluidics utilizes compartmentalization of single cells in droplets to enable the analysis of proteins released from or secreted by the cells. Microwells and pillars essentially trap the single cells facilitated by cell surface modification. Finally, laser capture microdissection can harvest the cells of interest directly by cutting away unwanted cells to give histologically pure and enriched cell populations. Although these methods can isolate single cells for analysis, they passively capture the cells and do not have three dimensional grip control.

In addition, capture and analysis do not happen on the same platform. Usually the capture method needs to be coupled with a separate analysis tool. To mitigate these problems, we designed and fabricated self-folding single cell grippers inspired by the previous studies in our lab using self-rolling thin films.[22,23,24,25]

2.1 Design and fabrication of the single cell microgrippers

As the size of microgippers got smaller (by a factor of approximately 30 compared to thermally-responsive biopsy grippers), the established fabrication methods and materials became insufficient for achieving a satisfactory folding angle, also related to the radius of curvature of gripper arms. In addition, we anticipated that our single cell grippers could reach tighter spaces in the body such as capillaries, alveoli, and the central nervous system, unlike the previous microgrippers that were used for biopsies on tissues.

Because of the electronic and physical properties of Si and its oxides (SiO and SiO_2), they have been used in many small devices for biological analysis and proven to dissolve in biofluids.[33,34] We confirmed the dissolution of the SiO and SiO_2 films in phosphate buffered saline (PBS) at 37°C [FIGURE 9].[35] It took 20 days for a 8 μm thick SiO film to dissolve whereas a 24 μm thick SiO_2 took 15 days. They are transparent, bioresorbable, biocompatible, and compatible with current MEMS processes. It was previously shown that bilayers of SiO and SiO_2 can be deposited at nanoscale thicknesses using an electron beam (e-beam) evaporation method and show radii of curvature in microscale.[36] Therefore, we decided to use these materials for the bilayer in addition to the rigid segments made up of SiO to fabricate self-folding single cell grippers.[35]

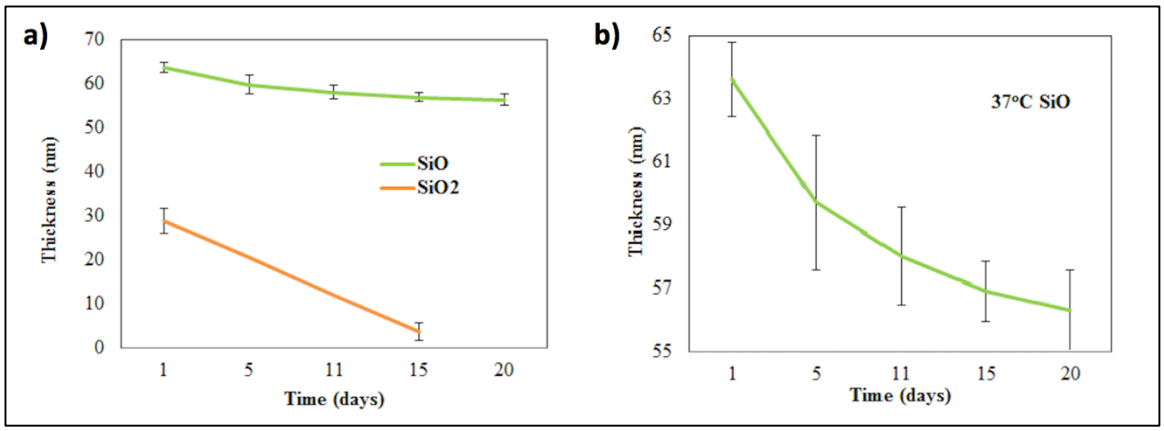

Figure 9: a) A graph showing the dissolution of SiO and SiO2 films over days and b) showing only the SiO film zoomed in. Dissolution of SiO2 was observed to be faster than the dissolution of SiO in PBS at 37°C. (Copyright © 2014 American Chemical Society)

In the light of previous microgripper designs from our lab, our new single cell microgrippers resembled a human hand with a palm but with only four fingers (arms). Each arm had two segments: a pre-stressed bilayer, which facilitated the folding, and a rigid segment, which facilitated gripping and controlled the folding [FIGURE 10]. The tip-to-tip size of the grippers ranged between 10 µm to 70 µm, and the thicknesses for SiO and SiO_2 bilayer varied accordingly. Depending on the application, the palm of the gripper was either attached to a Si wafer (array design) or lifted off completely (free-floating design).

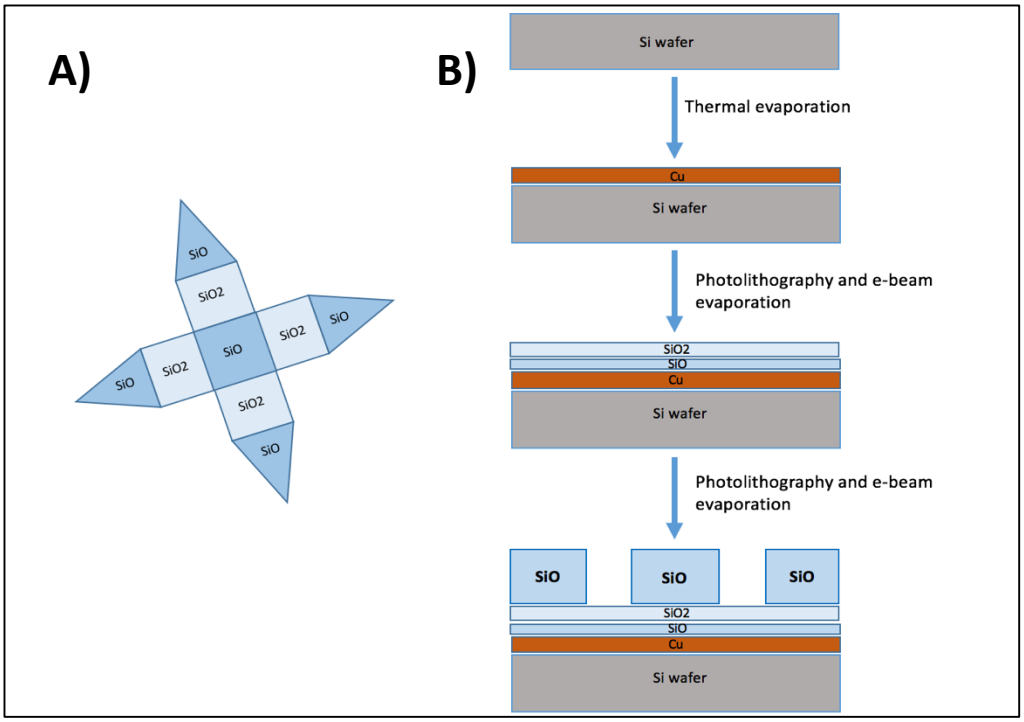

Figure 10: A) Top-view of a single cell microgripper showing the segments B) Fabrication of single cell microgrippers from a side view

We started the fabrication with a cleaned Si wafer (rinsed with isopropyl alcohol and water and dried with compressed air). For the arrayed design, we patterned the Cu sacrificial layer on to the Si wafer so that everywhere except the center of the grippers had Cu underneath. Then, we patterned and e-beam evaporated the pre-stressed SiO/SiO_2 bilayer in the shape of a whole gripper on the Cu layer. The gripper dimensions changed with the intended cell capture such that the center of the gripper had the area of a single cell. The thicknesses of the bilayers varied with the size of the gripper due to the restrictions in the folding angle [TABLE 1]. Due to this effect, we were able to control the folding angle by changing the thicknesses of the bilayer. These thicknesses provided folding angles between 90° and 115°.[35] We additionally used finite element analysis to

model stress measurements on the SiO/SiO_2 bilayer. The results showed the SiO film to be more compressive while the SiO_2 film to have more natural residual stress.

Gripper diameter tip-to-tip (µm)	Gripper Palm Length (µm)	SiO thickness (nm)	SiO_2 thickness (nm)
10	2	3	3
35	6.3	8	15
50	9	9	27
70	12.5	10	30

Table 1: Variation of the pre-stressed bilayer thicknesses with respect to grippers diameter (Copyright © 2014 American Chemical Society)

On top of the bilayer, we photo-patterned the rigid segments on the gripper arms and e-beam evaporated 150-350 nm SiO film. Finally, when immersed in the sacrificial etchant solution (either ammonium persulfate, APS-100, or phosphate buffered saline, PBS), the Cu layer dissolved and the gripper arms folded while their center palm remained attached to the wafer.

For the free-floating design, we thermally evaporated a Cu sacrificial layer everywhere underneath the gripper. Followed by the photo-patterning and e-beam evaporation of the bilayer (SiO/SiO_2) on top, we defined the rigid segments and deposited SiO with the same thicknesses mentioned above. The only difference in this design was the additional Cu sacrificial layer underneath the center of the grippers, which allowed the whole gripper to lift off from the wafer when immersed in the etchant solution [FIGURE 11]. With the free-floating design, we tested different hinge lengths (the bilayer between the rigid finger and the center) and different numbers of gripper arms to achieve

a satisfactory folding angle and uniform lift off of the grippers. For the 35 µm sized grippers, we tested 2.5, 3.5 and 5 µm hinge lengths and confirmed that a hinge length of 3.5 µm was most ideal for gripping and holding a single cell because it achieved a folding angle above 90°. In addition, a microgripper design with three flexible arms and 10 µm hinge length was tested. After lift off, it was proven to be not sufficient due to the collapse of the arms [FIGURE 12].

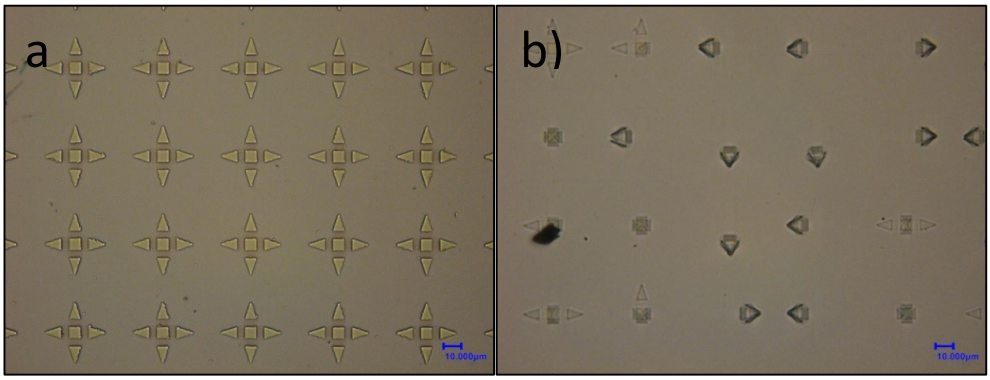

Figure 11: Optical microscopy images of a) 35 µm diameter grippers (with a hinge length of 3.5 µm) before lift off and b) after lift off in APS-100

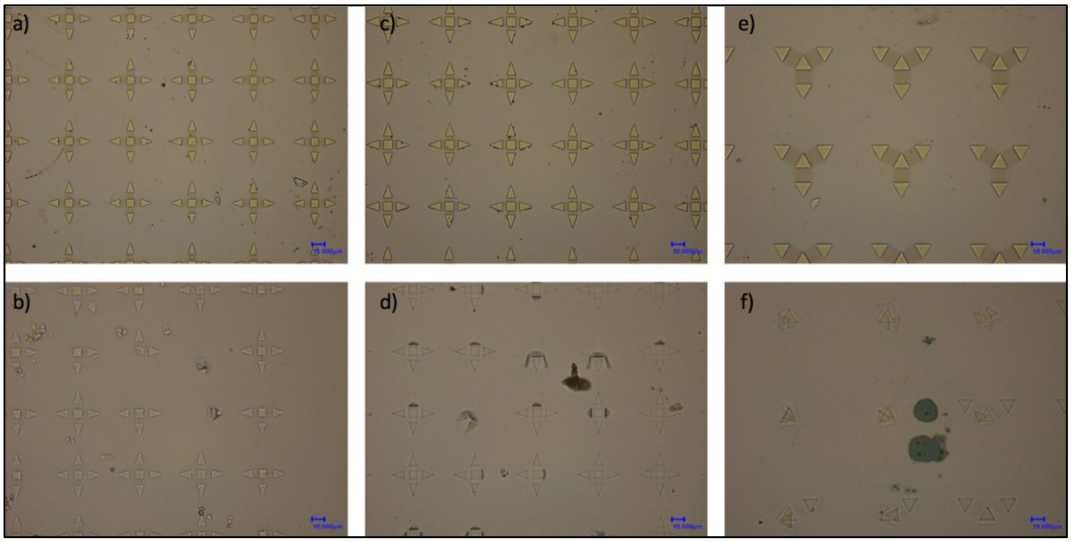

Figure 12: Before (above) and after (below) lift off images of 35 µm sized grippers with a-b) 5 µm hinge length, c-d) 2.5 µm hinge length, e-f) 10 µm hinge length with three arms

Given the small size of the gripper, we did not incorporate a controlled actuation mechanism (i.e. polymer trigger layer). The grippers closed and lifted off immediately when the Cu sacrificial layer was dissolved in the etchant solution. Instead, we optimized the etchant concentration (such as PBS, blood cells, and neutral red solution) to achieve a controlled folding of the arms in order to capture single cells.

2.2 Results and Discussion

2.2.1 Untethered capture of single cells

The free-floating design of the grippers allowed us to capture single cells, lift them off from the wafer, and move the grippers with the captured cells in solution. The purpose of this design was to show the moving capability of single cell grippers in an aqueous environment without losing the captured sample.

In this experiment, we used 35 μm diameter grippers with a total bilayer thickness of 20 μm to capture single red blood cells that were 8 μm in diameter. The gripper size was picked so that the center of the gripper would only contain one cell. After the fabrication of the gripper on a 3-inch Si wafer, we cut the wafer into smaller pieces that could fit in a small chamber on a microscope slide. The grippers were first soaked in 1% APS-100 etchant solution (in DI water) for 1 to 3 minutes. This step allowed the sacrificial layer underneath to start dissolving slowly. Once the arms were partially released, we rinsed the grippers with PBS. Then, a solution of PBS, Beagle red blood cells, and the neutral red dye (Marshall BioResources) was pipetted into the small chamber using the capillary action between the cover glass slide and the chamber walls [FIGURE 13].

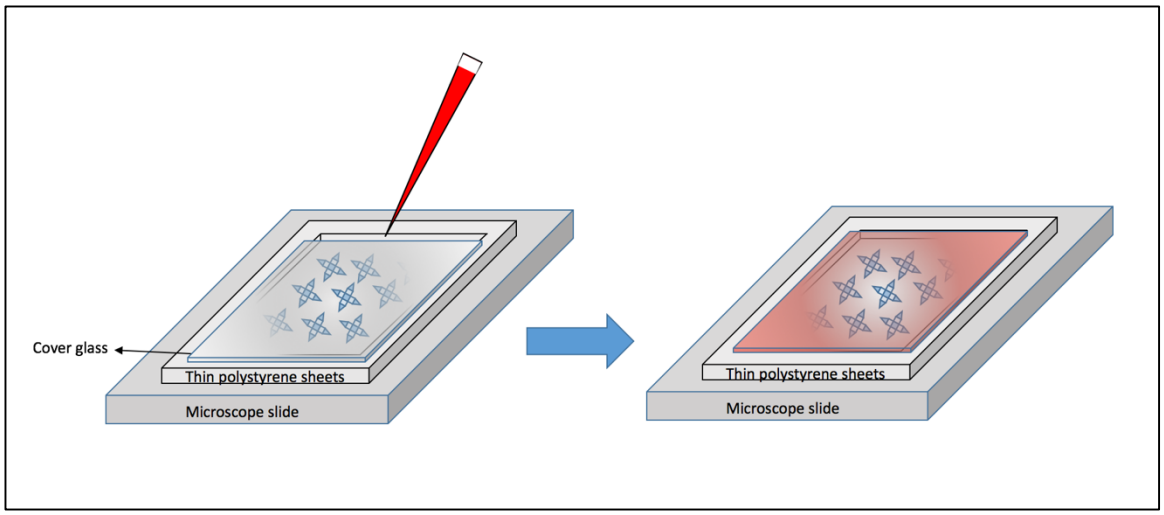

Figure 13: Experimental setup and the addition of red blood cells onto grippers using the capillary action between the grippers and the cover slide

We prepared the cell solution by mixing two drops of (35-50 µl) beagle red blood cells into 10 ml PBS with six drops (75-100 µl) of neutral red cell coloring agent. We kept this mix in the fridge for 15 minutes before the capture. Then, we mixed this cell solution with 1% APS in DI water. The optimum concentration for this mix was found to be 85% cell solution to 15% APS solution whereas the lower limit was 50% cell solution. Above the optimum concentration, the cells landed on top of each other rather than uniformly spreading over the gripper area. When multiple cells got seeded on the center of the gripper, they prevented the gripper arms from closing properly due to their weight [FIGURE 14]. After one to two hours, all of the grippers were closed properly and many of them were able to trap red blood cells within their grip. Following the closing of the arms, the grippers also lifted off completely from the Si substrate and floated in the solution with the captured cells. The capture of the cells was confirmed with optical microscopy and profilometry [FIGURE 15].

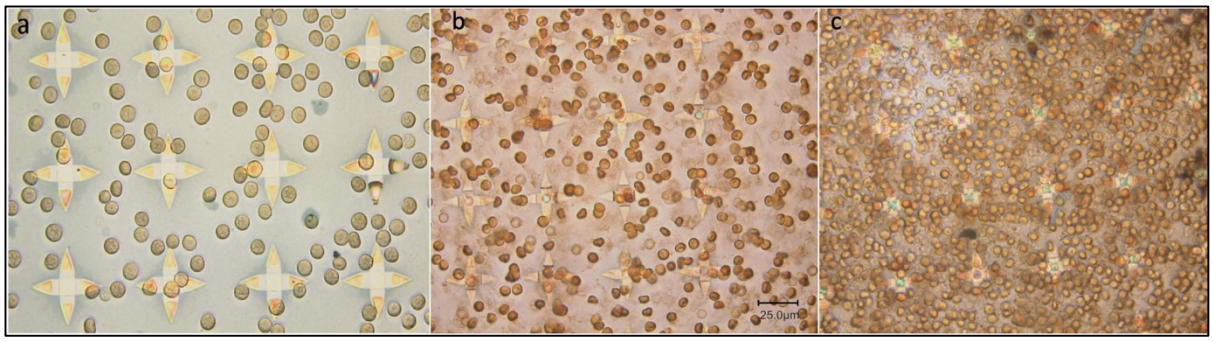

Figure 14: Optical microscopy images. a) Optimum cell concentration (3.5 µl blood/ml cell solution) during lift off of the gripper arms (Copyright © 2014 American Chemical Society) b) Crowded cell concentration (75 µl blood/ml cell solution). c) Over crowded cell concentration (200 µl blood/ml cell solution).

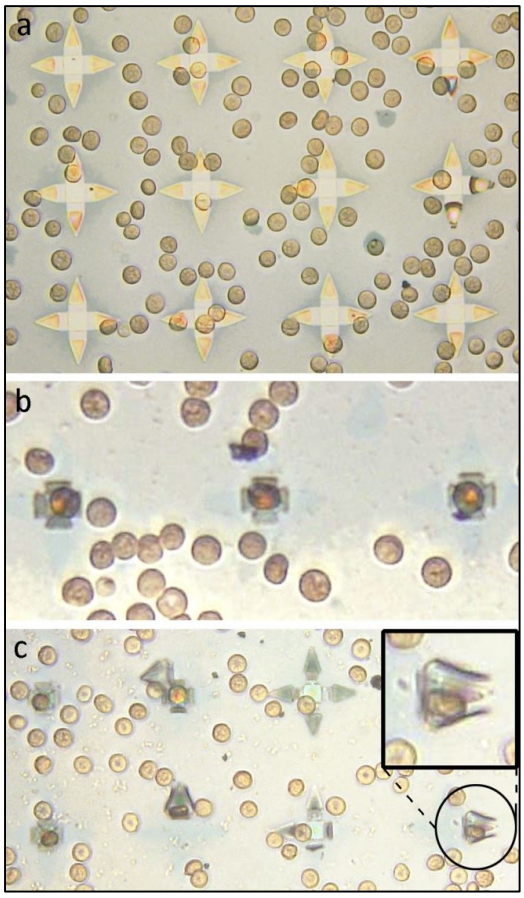

Figure 15: Optical microscopy images of the grippers a) before closing b) after closing c) after lifting off completely (Copyright © 2014 American Chemical Society)

As a result, our design and experiments supported the concept that these free-floating single cell grippers can be utilized as an in vivo cell capture tool within the hard-to-reach places in the human body such as capillaries, the urinary tract, alveoli, and the central nervous system. Due to the advantageous properties of SiO and SiO_2 such as transparency, biocompatibility, and mechanical flexibility, we were able to fabricate these grippers, capture single red blood cells, and maintain the captured cell while floating in an aqueous environment. With the addition of a magnetic thin film layer (i.e. highly stressed bilayers of Ni) within the arms, maneuverability can be achieved within these tight places [FIGURE 16]. This technique can also be applied in biopsy and drug delivery in a specific region. In order to achieve these, we must incorporate an actuation layer (i.e. a polymer such as hydrogel or paraffin) on the hinge regions that can be loaded with the desired drug molecules. The polymer layer works as a neutralizing force on the bilayer, keeping the arms open even after the dissolution of sacrificial layer.

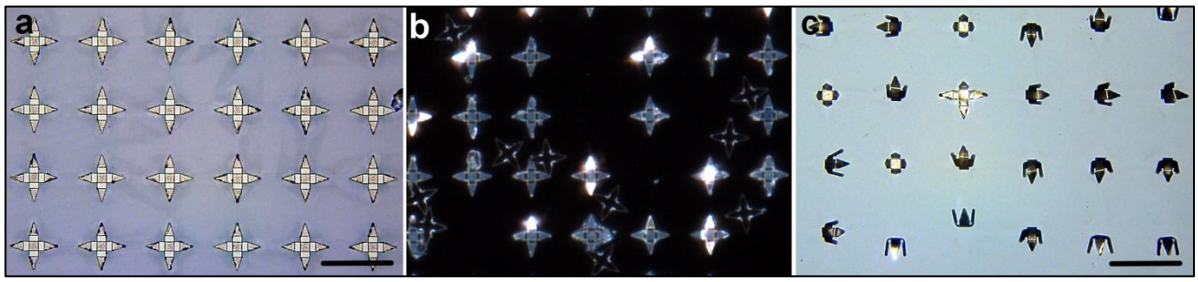

Figure 16: Optical microscopy images of 70 μm sized microgrippers, made up of a Ni/Ni bilayer and a paraffin hinge trigger layer. a) Prior to the release from Si wafer. b) After the release from Si wafer. c) After the trigger with a folding angle of 85°. (Scale bars are 100 μm) (Copyright © 2014 ACS)

2.2.2 Tethered capture of single cells

The ingenious design of these microgrippers not only allowed them to be used as in vivo single cell capture tools, but also made them suitable for an in vitro biological analysis device in an arrayed form. Micro-sized analytical devices are proven to be high throughput compared to macro-sized systems, and these grippers provided yet another example for this. Attached by their centers to the Si substrate, the three dimensional design of the gripper arms was able to trap, assay, sustain and allow imaging of single cells with a high yield.

Initially to demonstrate the arrayed capture and analysis, we utilized 50 μm sized (tip-to-tip) grippers with 40 μm bilayer thickness and performed L-929 mouse fibroblast single cell capture.[35] Similar to the experimental set up shown in Figure 13, we cut the Si wafer with gripper features into smaller pieces to fit them in a small chamber attached to a glass slide. With the help of capillary action, we pipetted the cells in media solution into the chamber. The dissolution of the Cu sacrificial layer, which was deposited everywhere except the center of the grippers, was relatively slow compared to the traditional Cu etchant (APS-100). It took the grippers between 2-6 hours to close in the incubator. The solution was in a warm (37°C) cell culture media, which included ions that slowed down the etching reaction. However, the absence of the APS etchant in this experiment was necessary for the future assays planned for the cells because it is a strong oxidant, which can kill the cells. Following the capture, we rinsed out the untrapped cells in the environment with clean media.

After the capture, the viability of the cells was confirmed with a calcein AM fluorescent viability test (green fluorescent meaning viable) and the capture was

additionally confirmed with scanning electron microscopy [FIGURE 17]. Due to the transparency of the SiO and SiO_2 layers, we were able to optically confirm that there were cells in the grippers and fluorescent imaging was possible through the arms. In an area of 75 microgrippers, we achieved a capture yield of 48% and all the captured cells were alive. Just like the free-floating gripper design, the closing of the arms was affected by the cell concentration due to the force that excess cells exert on the arms. The best performance of capture was observed when there was a maximum of two cells touching one microgripper so that the gripper could capture a cell but not more.

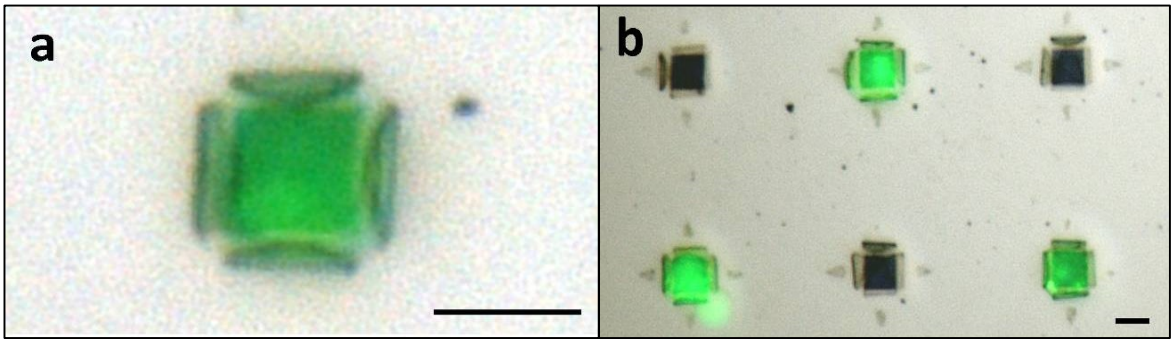

Figure 17: L-929 mouse fibroblast capture with 50 µm sized grippers. a) A viable captured cell b) Capture yield over a region (Scale bar is 10 µm) (Copyright © 2014 American Chemical Society)

Additionally, we tested our grippers with a different cell line and gripper size. We utilized metastatic human breast adenocarcinoma cells (MDA-MB-231) in order to be able to further use our grippers in cancer detection assays. For the capture of a single breast cancer cell, we designed and fabricated 70 µm (tip-to-tip) grippers, which were small enough to trap one cell only. The fabrication and the experimental set up were the same as the 50 µm size grippers. We confirmed the capture of cells both optically and with scanning electron microscopy (SEM) after fixing the cells according to the protocol

by Perkins and McCaffery.[37] After the capture, we rinsed the untrapped cells with fresh and warm media, and removed the gripper piece from the chamber into a 3% formaldehyde solution with 1.5% glutaraldehyde in 0.1M NaCacodylate. We fixed the cells at room temperature for one hour. After we washed and post-fixed cells with Palade's OsO_4 for one more hour, we dehydrated the trapped cells in series of cold (4°C) ethanol (15 minutes each in 70%, 90%, and 100%). Following the dehydration, we performed a critical point drying method to completely dry the trapped cells. The critical point drying was necessary because of the high surface tension (γ_{LG}) forces of ethanol on the closed gripper arms [FIGURE 18]. When we let them air dry in ethanol, we observed the arms opening back up due to this effect. Finally, cells were ready for SEM imaging between 1.5-10 kV.

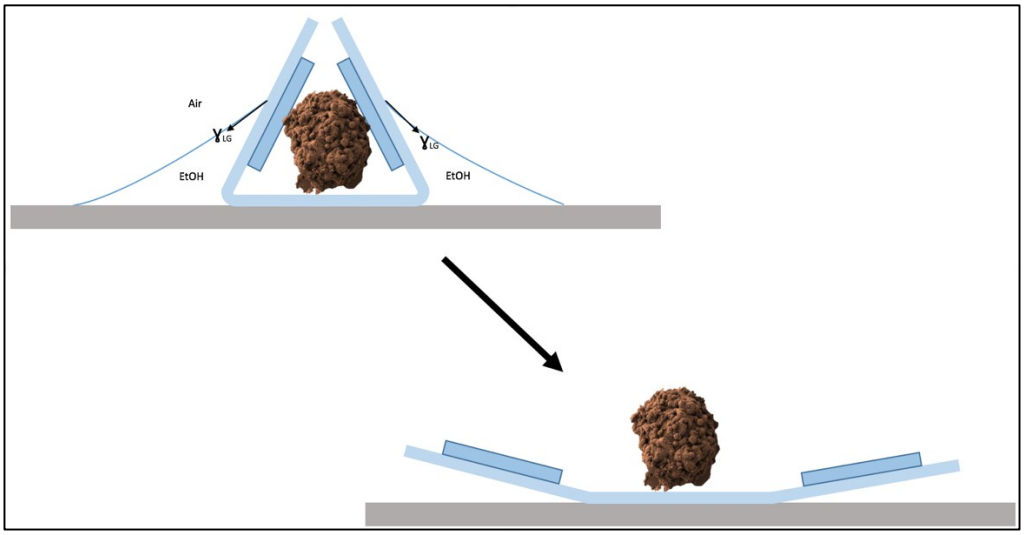

Figure 18: Surface tension force of ethanol on the gripper arms. If air dried, the spring force on the gripper arms due to the residual bilayer stress cannot overcome the surface tension force, and consequently the arms open up.

In addition to the size difference, we also varied the shape of the arms to find a more convenient design to observe the trapped cells [FIGURE 19-21]. Square-shaped arms provided a better visual of the trapped cells due to the geometrically open top, whereas the triangle-shaped arms trapped the cells more tightly and only allowed the surrounding media through the openings between the arms. To further confirm, we took SEM images of untrapped MDA-MB-231 cells after fixing [FIGURE 22]. Tight capture was desired so the sample would not fall out when the wafer piece was inverted for further analysis. Because of this, the difference in arm shape only mattered when the size of the cell changed.

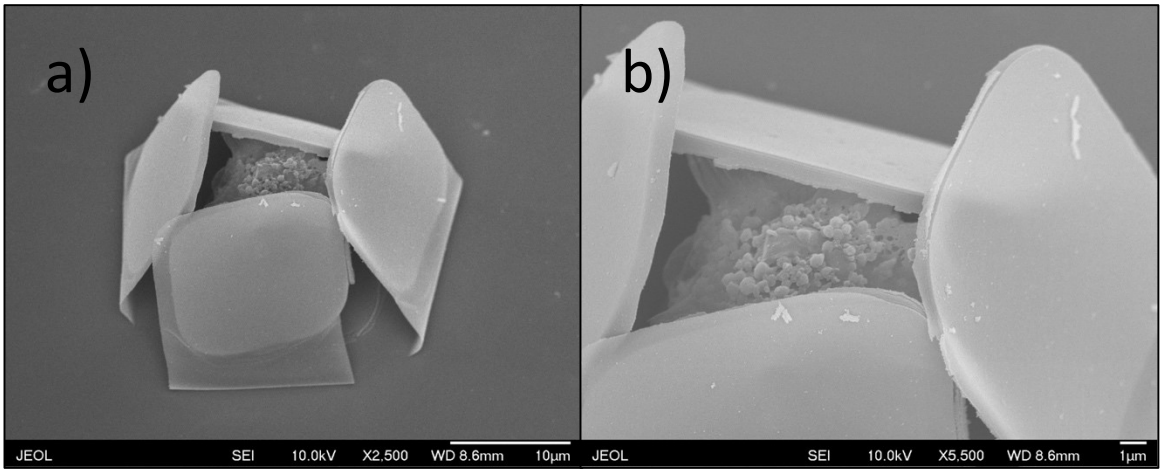

Figure 19: a) SEM image of a trapped MDA-MB-231 cell in a 50 µm gripper. (scale bar: 10 µm) b) Zoomed in image of the trapped cell in the same gripper. (scale bar: 1 µm) The accelerating voltage for the images was 10 kV.

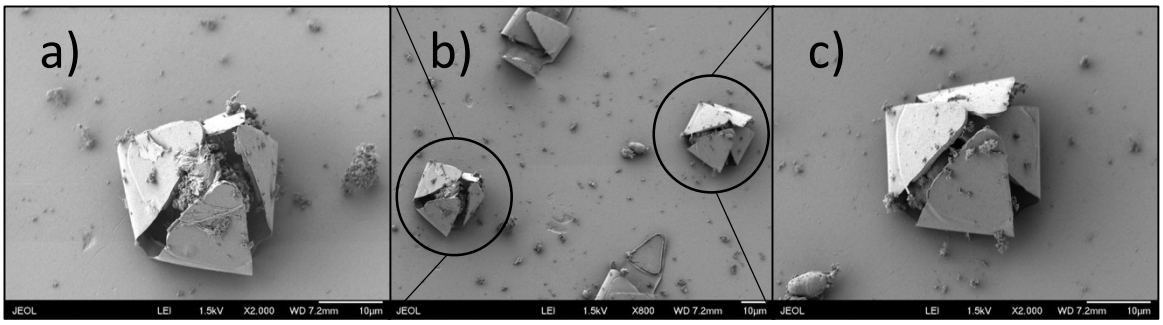

Figure 20: a) SEM image of a trapped MDA-MB-231 cell in a 50 µm gripper. (Material in process for publication) b) Trapped cells over an area of four grippers. c) Zoomed in image of a trapped cell in the area shown in (b). Scale bar for the images was 10 µm.

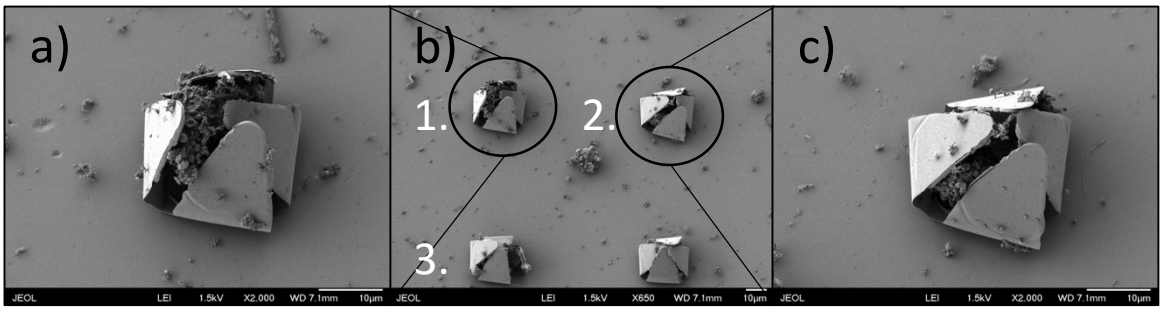

Figure 21: a) SEM image of a trapped cell in a 50 µm gripper on the area shown in (b). b) Three trapped cells over an area of four grippers. (Material in process for publication) c) Zoomed in image of a trapped cell in the area shown in (b). Scale bar is 10 µm.

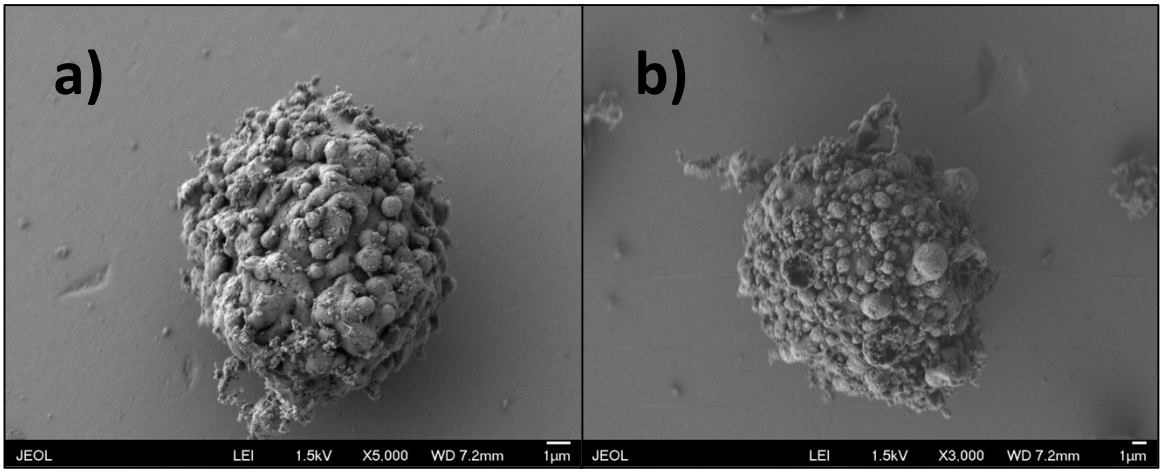

Figure 22: (a-b) SEM images of untrapped, fixed, and critical point dried MDA-MB-231 cells. Scale bar is 1 µm and the accelerating voltage is 1.5 kV in each image.

2.2.3 Plasmonic systems for diagnosis

In addition to the fluorescent cell viability test, there are a variety of analysis techniques that can be done after cell capture on an array of microgrippers. Our collaboration with the Mechanical Engineering Department (Professor Ishan Barman and Dr. Ming Li) allowed us to carry a surface-enhanced Raman spectroscopy analysis on the captured human breast cancer cells.

Screening the cellular processes plays an important part in observing normal tissue development and advancement of diseased tissues. These cellular processes, which cause phenotypic and genotypic differences between healthy and cancer cells, are guided by molecular signals. The molecular signals trigger upstream or downstream molecular events that lead to a characteristic property (blebbing, cell shrinkage, DNA fragmentation, etc.) of a cell.[38] Traditionally, these molecular activities can be followed with fluorescent microscopy, however fluorescent probes are prone to photobleaching, and they face overlap issues of the emission bands.[39,40,41] A Raman signal has a peak width of 1-2 nm whereas a typical fluorescent (from organic dyes, etc.) emission peak width is 10-100 times wider, which restricts the resolution of the analysis for simultaneous molecular processes within a cell.[42]

Recently, plasmon-enhanced Raman spectroscopy (also called surface-enhanced Raman spectroscopy, "SERS") matured to be used as a single molecule detection system, compared to the traditional Raman spectroscopy method in which there were no enhancement substrates such as metallic nanoparticles.[43,44] When surface plasmons, which are clouds of oscillating free electrons from the metal nanoparticles, get excited by the incident light at a certain frequency (visible or near-infrared radiation), they resonate

with the radiation. This resonation causes field enhancement in the incident light and leads to increased signal of the Raman scattering from the molecule of interest.[45] Hence, if a biomolecule is coupled with a metallic nanoparticle under Raman spectroscopy, the weak Raman signals from the biomolecule can be enhanced and show a distinct peak for that biomolecule in the spectroscopic graph. This way, it is possible to collect characteristic properties from a single cell on a molecular level.

In order to use SERS for single molecule detection with our grippers, we needed to coat the inner surface of the grippers with a uniform layer of metallic nanoparticles. In their previously published work, our collaborators, Prof. Barman and Dr. Li, investigated the Raman signal enhancement factors of gold nanostars (AuNS) and found that an optimum nanostar concentration is needed to maximize the enhancement factor (EF) [FIGURE 23].[46] The tips of the nanostars behaved as so called “hot spots” and helped to enhance the incident light, hence the Raman signal. They utilized a non-fluorescent Raman reporter molecule, 4-nitrobenzenethiol (4-NTP), to attach onto the AuNS and used a laser excitation at 785 nm to observe the distinct -O-N-O bond peak on the SERS spectrum at 1342 cm^{-1}.

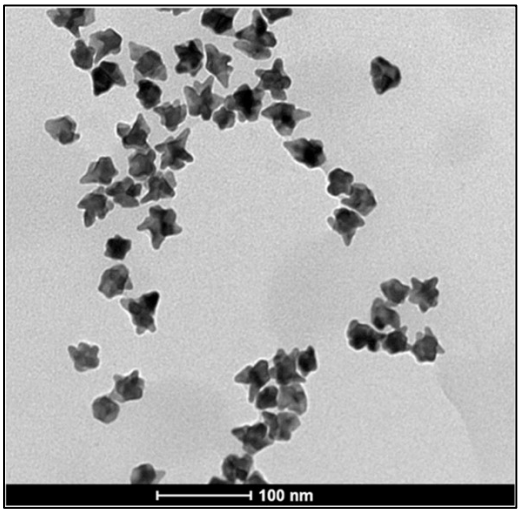

Figure 23: Transmission electron microscopy (TEM) image of gold nanostars with a diameter range of 25-30 nm (Material in process for publication)

The fabrication of the grippers for the SERS analysis was the same as the arrayed design with attached centers of the grippers. However, we used a quartz wafer substrate, which is transparent, instead of a Si wafer substrate (opaque) to be able to take the Raman images of the 3D structure of captured cells. We deposited a 30 nm thin film of germanium as the sacrificial layer everywhere except the centers of the grippers. This layer dissolved in pure water at warm temperatures (50-60°C), and prevented the cells from dying during the self-folding of the arms. Then, we photopatterned the stress layer (10 nm SiO/15 nm SiO_2) in the shape of a whole gripper. Next, we deposited 200 nm SiO_2 on the rigid panels on the arms [FIGURE 24].

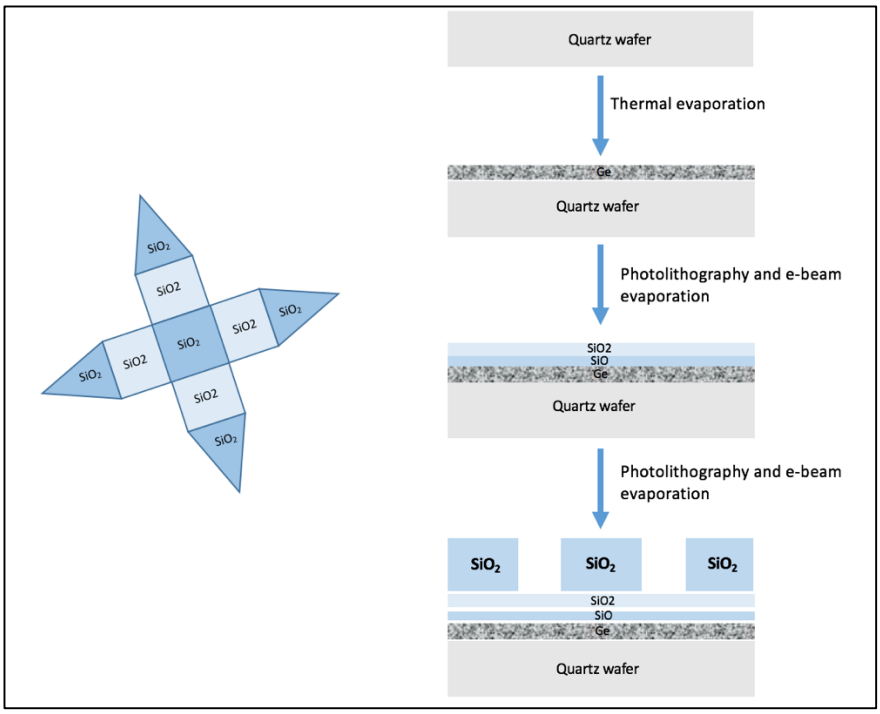

Figure 24: Schematic of the fabrication steps for microgrippers for the SERS analysis and imaging.

Subsequently, we cleaned the surface of the grippers with an O_2 plasma etch and washed with ethanol, which exposed –OH groups on the surface. After the immersion of the grippers in a 50 mM (3-aminopropyl)triethoxysilane, APTES, solution (in ethanol) for one hour, we washed the excess silane molecules with pure ethanol. At the end of this step, the functional end of APTES ($-NH_2$) was exposed. We then incubated the grippers in a sonicated solution of 0.5 nM AuNS (25-30 nm in diameter, in ethanol) on a shaker with 200 rpm for 2 hours. Taking advantage of the amino group ($-NH_2$) and gold (Au) binding affinity, we ended up with a uniform layer of gold nanostars on the grippers with a density of moer than 100 nanostars/μm^2 [FIGURE 25]. We confirmed the gold nanostar coating on the arms with SEM imaging [FIGURE 26].

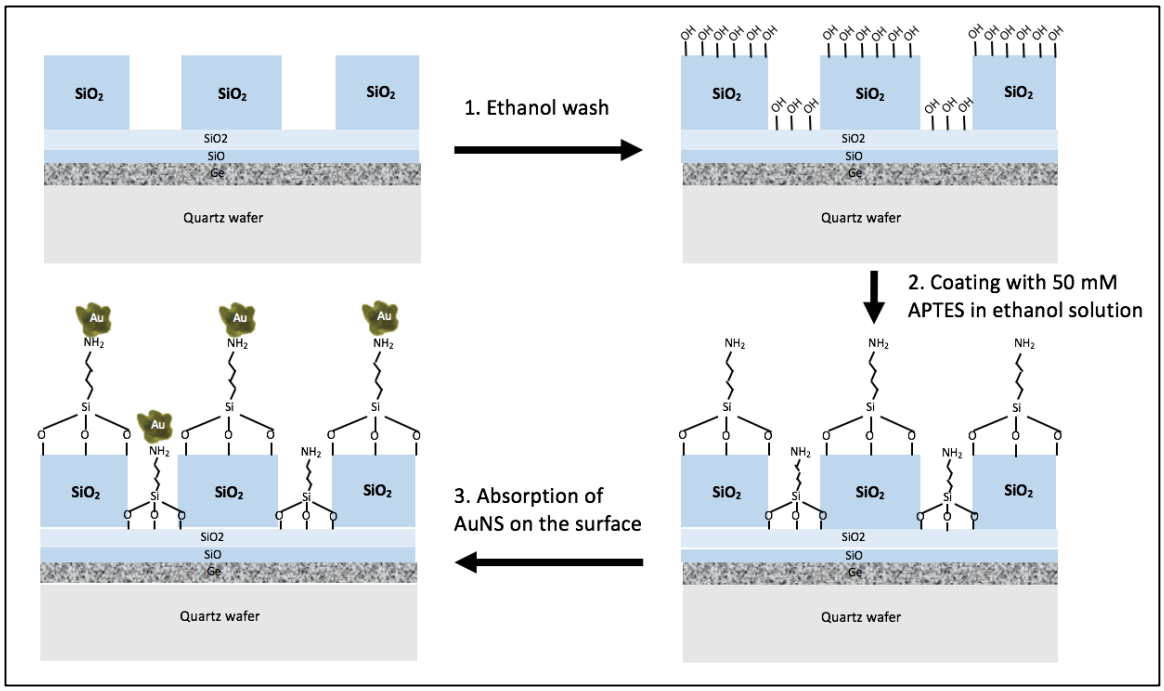

Figure 25: Schematic of the surface modification on microgrippers with gold nanostars before cell capture for SERS analysis.

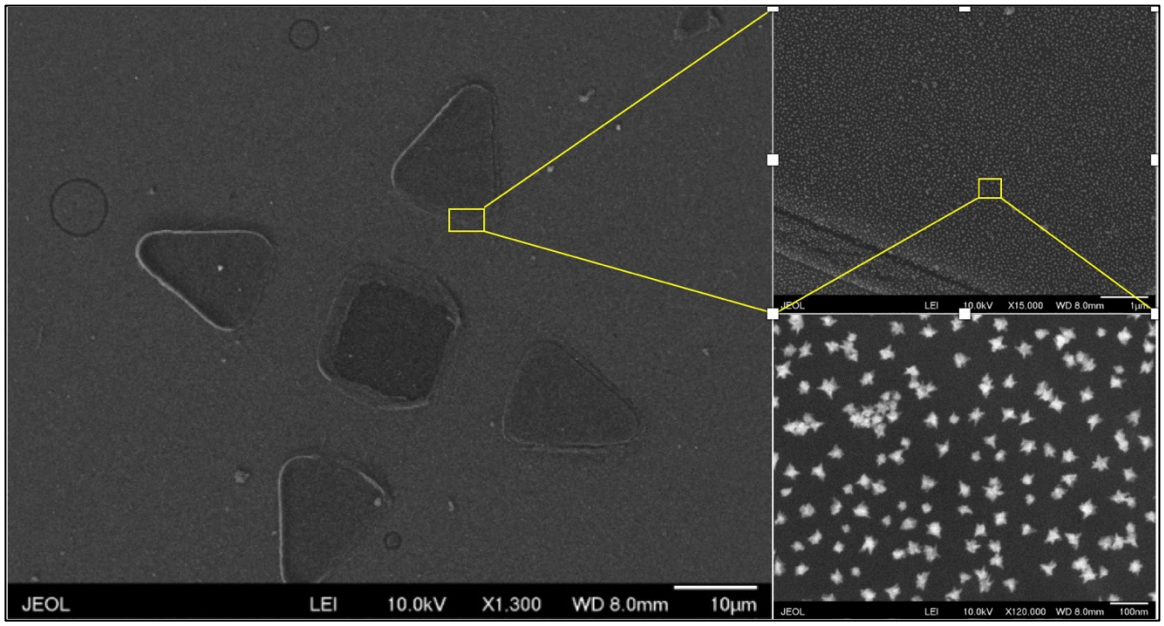

Figure 26: SEM images of AuNS coated grippers. Images to the right are zoomed in captures of the gripper arm and the uniformly coated nanostars on top. (Material in process for publication)

Before testing the effectiveness of the AuNS layer on the human breast cancer cells, we performed a proof of concept experiment by partially modifying the surface of Janus-like glass beads with AuNS and 4-NTP Raman reporter molecule that binds to the Au modified regions only [FIGURE 27]. 4-NTP has a molecule-specific Raman signal peak at 1342 cm^{-1} due to the –O-N-O band stretching in its molecular structure. Therefore, we observed an enhanced NTP Raman signal at 1342 cm^{-1} at the gold coated areas more so than other areas. This result was attributed to the field enhancement of the localized surface plasmons resonance from the gold nanostar surface, creating "hot spots". We also carried out a dynamic chemical analysis on the beads by breaking the Au-S bonding between the 4-NTP and nanostars using an oxidant such as APS-100 or H_2O_2 [FIGURE 28]. As the oxidants broke the bonds, we observed weaker intensity for the 1342 cm^{-1} peak for the NTP molecule, which proved that the signal enhancement was due to the AuNS coupling.

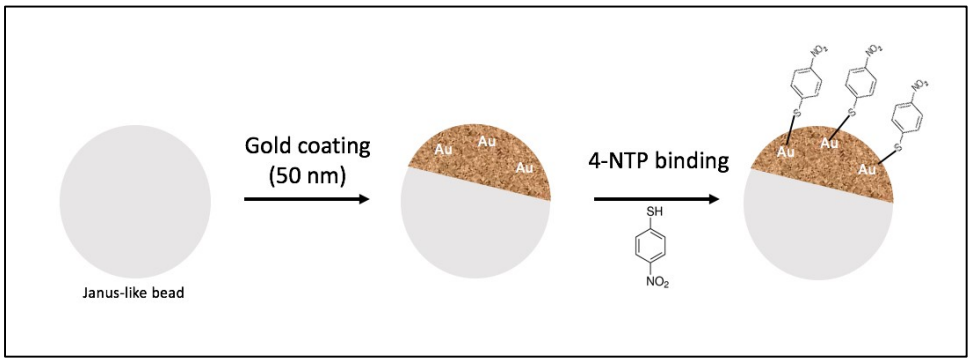

Figure 27: Chemical process of 4-NTP binding on to Janus-like beads with 30 μm diameter.

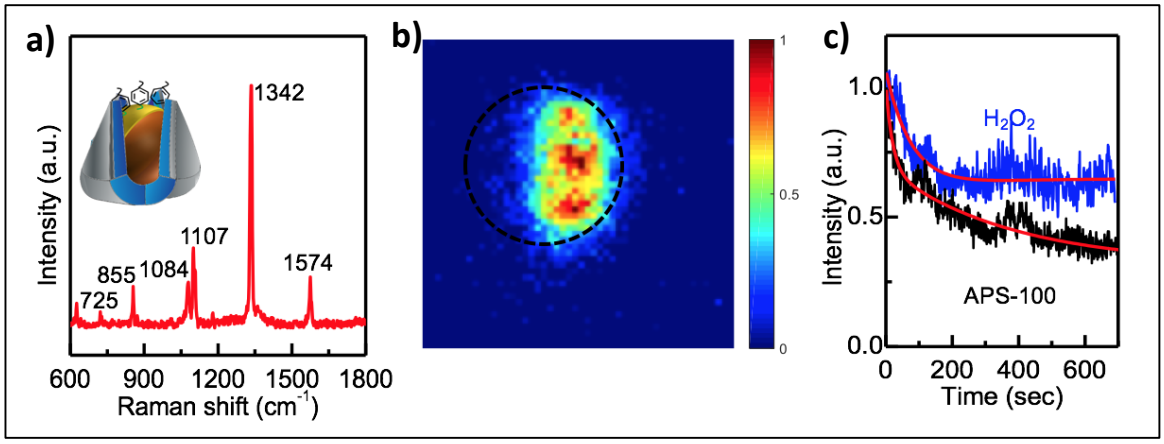

Figure 28: a) SERS spectrum of a trapped Janus-like bead. The SERS intensity is normalized by the maximum SERS intensity at the 1342 cm-1 band. (power: 63 mW, integration time: 1 s) b) SERS image of the trapped bead. Only the gold coated region showed a strong SERS signal due to enhancement. The SERS image is constructed using the integrated 1342 cm^{-1} band intensity of O-N-O bonding. (50x50 pixels over 80x 80 um area). c) Dynamic SERS analysis of 4-NTP (at 1342 cm^{-1}) during the bond breakage after adding the oxidants. (Material in process for publication)

With this initial confirmation, we moved on to apply SERS to captured MDA-MB-231 cells. After the fabrication and the AuNS modification of the grippers, we placed the gripper pieces in a 12-well plate and added 2 mL of pure water in each well. We accelerated the Ge sacrificial layer dissolution in water at 60°C for 30 minutes. After about 30 minutes, we placed the gripper pieces in fresh cell culture media and added 1 mL of the human breast cancer cells (dilution of 9/10 from a 90% confluent cell culture flask). We let the cells settle and placed the plate back into the incubator overnight for complete dissolution of the sacrificial layer under the arms. This way, during the closure of the arms, the cells were still alive. We visually confirmed the capture of the cells using optical microscopy, and then transferred the gripper pieces with captured cells into our small chamber with microscope slides. After covering the top with a cover slide and adding additional fresh cell culture media into the chamber, we placed the chamber set-up on the Raman laser for analysis. With the help of our collaborators, we carried out a 3D

profiling of the single molecules in the captured cell at the distinct Raman peaks for lipids (1456 cm^{-1} from –C-H bonding) and nucleic acids (1090 cm^{-1} from –O-P-O bonding). The Raman scanning started from the bottom of the gripper and acquired data every 5 µm up to 15 µm [FIGURE 29].

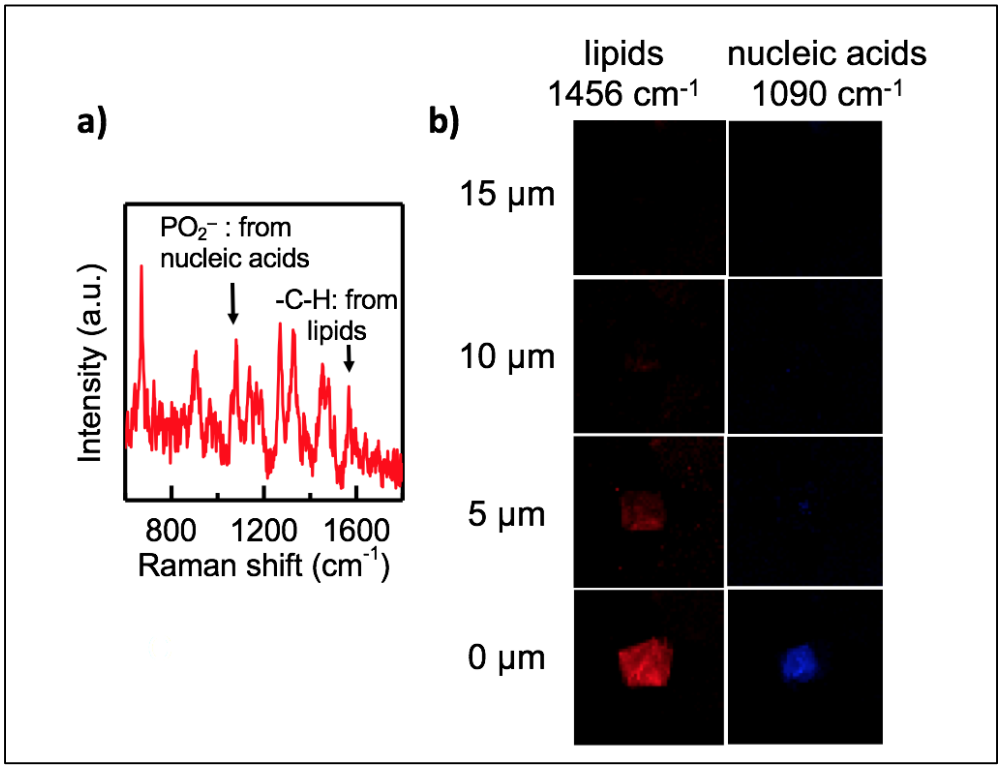

Figure 29: SERS multiplex imaging and 3D single molecule profiling. a) Representative SERS spectrum of the trapped cell. b) 3D single molecule profiling of live single cell for lipids at 1456 cm^{-1} band and nucleic acids at 1090 cm^{-1} band. (power: 5 mW, integration time: 1 s, 50x50 pixels over 80x80 µm area) (Material in process for publication)

We further confirmed the Raman signal enhancement effect of AuNS by capturing MDA-MD-231 cells with grippers without nanostars and with nanostars and performed SERS analysis on both [FIGURE 30]. Compared to grippers with AuNS coating, we didn't see any distinctive Raman signal from the grippers without any coating. The Raman signal from a bare cell was too weak to detect, especially when the

near-infrared laser was used as the incident light. However, when the AuNS on the grippers had contact with the cell membrane, the hot spots on the star tips caused enhancement of the signal at that point and showed a distinguishable peak. It was, therefore, important to have a uniformly coated layer of AuNSs on the gripper arms to ensure that after capture, the arms are tightly closed around the cell and the AuNS layer is in contact with the cell.

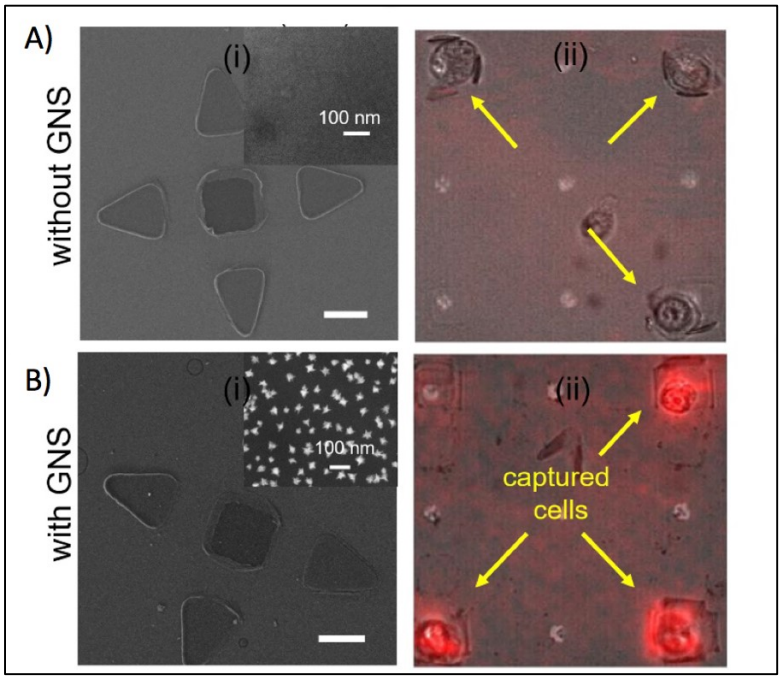

Figure 30: Label-free detection of single molecules in MDA-MB-231 cell using SERS. a) (i) SEM image of the grippers without any AuNS-modification (scale bar: 10 µm). The inset shows a zoomed in area on the gripper. (ii) Overlaid SERS image of a 4x4 gripper area with three captured cells. b) (i) SEM image of the grippers with uniformly coated gold nanostars (scale bar: 10 µm). The inset shows the nanostars on the gripper. (ii) Overlaid SERS image of a 4x4 gripper area with three captured cells. The SERS images are constructed using the integrated intensity of –C-H deformation band (1456 cm^{-1}, shown in red) and the intensity is normalized with the maximum SERS intensity in the data set. (power: 36 mW, integration time: 1 s, 100x100 pixels over a 160x160 µm area) (Material in process for publication)

As a result, we proved that our microgripper design can be used not only for a fluorescent viability assay but also for chemical profiling at a single cell level. The arrayed design helped capture the cells and keep them in a specific location through which a laser was excited to collect Raman signals from known band peaks of distinct bonds. In our experiments, we knew what the captured cells were and that we expected to see peaks at 1456 cm^{-1} (–C-H deformation bond in lipids) and at 1090 cm^{-1} (–O-P-O bond in nucleic acids). However, this assay with grippers and SERS can be done with a mixed culture of cells. After capturing the different cells in grippers, it is possible to get an enhanced Raman spectrum and identify the peaks accordingly in order to study the cell heterogeneity. Since biomolecules are abundant in the cells and crucial for the living, observations on growth and metabolism of healthy and diseased cells can be made. In addition, since grippers and SERS do not harm the cells and can be carried out in aqueous environment, this method can be used as a monitoring tool for the vesicles that are used for drug delivery. This analysis can provide a result of Raman signal intensity over time for the peak corresponding to a drug molecule. Hence, we can better understand the drug metabolism of the cell.

2.3 Conclusion and future work

In summary, we designed and fabricated microgrippers at the single cell level to capture and isolate them from a solution without harming or killing them, and then we applied different assays. We fabricated these grippers using microfabrication techniques in 2D (thermal and e-beam evaporation, lithography, O_2 plasma etching, etc.) and biocompatible, optically transparent materials (SiO/SiO_2, and gold nanostars). The unique

design with sacrificial layer contributed to the 3D self-folding without applying any outside energy into the system. By employing different sizes and shapes of these grippers, we were able to adapt them to any cell type and provided examples with mouse fibroblasts, Beagle red blood cells, and metastatic breast cancer cells. We also varied the sacrificial layer design to create tethered and untethered grippers on Si or quartz wafers for uses in vitro and in vivo, respectively. Utilizing the in vitro arrayed design, we accomplished a fluorescent viability test, and a SERS analysis/imaging on the captured cells to detect single biomolecules inside the cells. We confirmed the captures with both live optical imaging and with fixed cells using SEM imaging. Our work here provides a proof of concept and is open to any modification.

Future studies could investigate including an actuation mechanism in the current design of single cell grippers. Thermal, chemical and optical actuation mechanisms have been previously studied and applied in our lab on the biopsy grippers, hence we could try to incorporate these systems into our single cell grippers. For example, addition of a thermo-responsive polymer on top of the grippers (either on the whole area or only on the flexible hinges), such as paraffin wax, can give control over the actuation of the arms with respect to temperature. Or, we can use gelatin, a polypeptide, or carboxymethylcellulose (CMC), a polysaccharide, as the trigger layer that can get enzymatically actuated when exposed to proteases or glucosidases respectively. For the in vivo applications, metal thin films with ferromagnetic properties (i.e. Ni) can be deposited on the rigid panels to add control over the motion of the grippers in a biological environment. Last but not the least, we can modify the surface of the grippers to make them specifically capture one type of cell in a mixed culture. To do this, we can

functionalize the surface of the grippers with antibodies distinctly corresponding to a cancer cell membrane protein. For example, in human breast cancer cells, it is observed that herceptin-2 is an abundant receptor and cause of the malignant behavior.[47,48] Therefore, attaching antibodies that will target the herceptin-2 molecule on the surface can lead to the capture of only the breast cancer cells in the solution or in the tissue. This application can converge with the field of drug delivery for therapy by loading the trigger layer (e.g. a hydrogel) with the desired drug. In conclusion, there are many ways to modify the microgrippers according to the application and the current design of the grippers provides ease in the adaptations to these applications.

Chapter 3: Thermally-responsive untethered microgrippers

Self-folding microgippers are not only effective on the single cell level, but also on the tissue level. With the development in microfabrication and robotics, surgeries and diagnostics desire minimally invasive techniques to be applied on patients. For example, traditional biopsies on suspicious lesions can be painful and can leave the patient in distress because of the tools that are used such as forceps. In addition, the current biopsy tools are not efficient and practical enough to screen large area organs (i.e. esophagus, colon, stomach, etc.) without missing a small cancerous region due to the size of the forceps, low negative predictive value, cost, and amount of distress they cause to patients at each tissue retrieval.[49] They also lack the surface coverage needed to confidently make a decision on precancerous lesions. In a study, it was shown that the negative predictive value of a biopsy with forceps was 4.7% in detecting esophageal adenocarcinoma, which indicates that the traditional biopsy can not predict the probability of a subject having the disease accurately.[50] Furthermore, they realistically can't screen the whole organ for precancerous lesions due to patient's comfort limits.

Previously in our lab, Gultepe et al. designed and fabricated self-folding thermally actuated surgical microgrippers with sizes varying from 300 μm to 1 mm and performed ex vivo and in vivo tissue sampling utilizing these grippers.[25,24,51,52] Again the cost effectiveness, mass producible fabrication and the tetherless manipulation of the grippers gained advantage over the traditional biopsy tools, where everything is controlled via external cords and energy sources. Although the tissue sampling studies by Gultepe et al. provided a statistical model, they lacked the real statistical sampling results of the microgrippers in a large area organ biopsy (e.g. esophagus in GI tract). Hence, the aim of

this project was to provide a resolution study for these thermally-responsive microgrippers by employing an in vivo statistical sampling in the gastrointestinal (GI) tract of a live animal (i.e. pig). We investigated a UV-visible dye to mimic a diseased area, the trigger layer material that can respond to temperature, and hydrophobicity of the gripper after lift off from the wafer.

3.1 Design of the thermally-responsive microgrippers

For the fabrication of the microgrippers used in this study, we followed the pre-determined recipe for the thermally-responsive microgrippers.[52] We started with a clean Si wafer by rinsing it with isopropyl alcohol and deionized water. We deposited a 100 nm thick Cu sacrificial layer after deposition of a 15 nm thick chromium (Cr) adhesion layer using thermal evaporation. Then, we photopatterned a stress layer everywhere including the center of the gripper using lithography techniques (photoresist S1827), and deposited a bilayer of 60 nm Cr followed by 100 nm gold (Au). This bilayer was the main cause of bending of the arms due to the residual stress between the two thin films. We, again, photopatterned the rigid panels on the arms (photoresist SPR220), and utilized electroplating to deposit a 5 μm thick nickel (Ni) layer sandwiched in between 0.5 μm Au layers [FIGURE 31]. In addition to this established protocol, we investigated a different trigger layer on top of the grippers to control the actuation with temperature. We spin coated two different polymers, paraffin wax and pluronic F-127 gel, and observed the layer coverage on the arms as well as the hydrophobicity of the grippers after the coating. The purpose of this trigger layer is to keep the arms flat until the grippers are in an environment at 37°C and above.

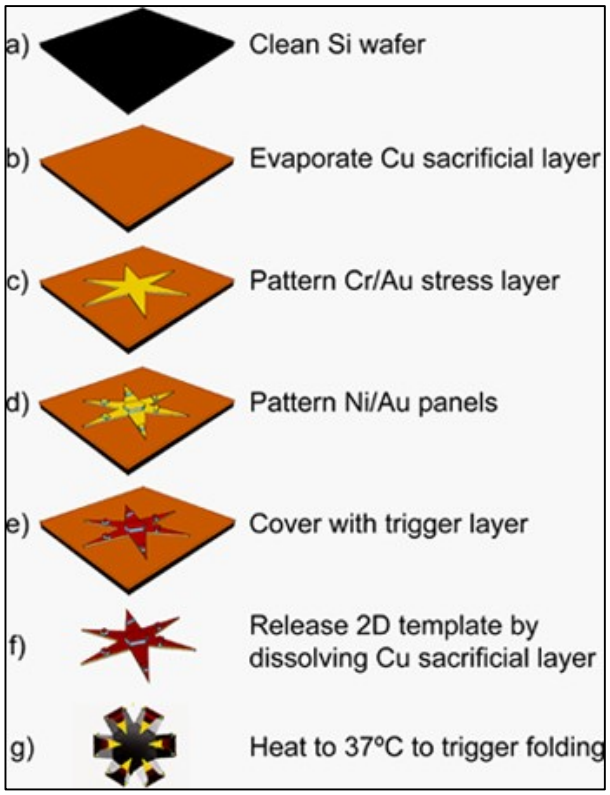

Figure 31: Schematic of the microfabrication steps for the thermally-responsive microgrippers (Pandey S., Gultepe E., Gracias D.H.)

The size of the grippers was adjusted to 900 µm from tip-to-tip so that it can grip on to a biological tissue and retrieve it from the tissue wall. Compared to the four-arm design in single cell grippers, these were made up of six-arms resembling a star-shape or a hand, and had two hinges in each arm to increase the gripping efficiency. We fabricated three different arm structures according to the protocol [FIGURE 32].[52] The rationale behind these different designs was to test the gripping strengths. However, we did not observe a substantial difference between the different design in terms of capture.

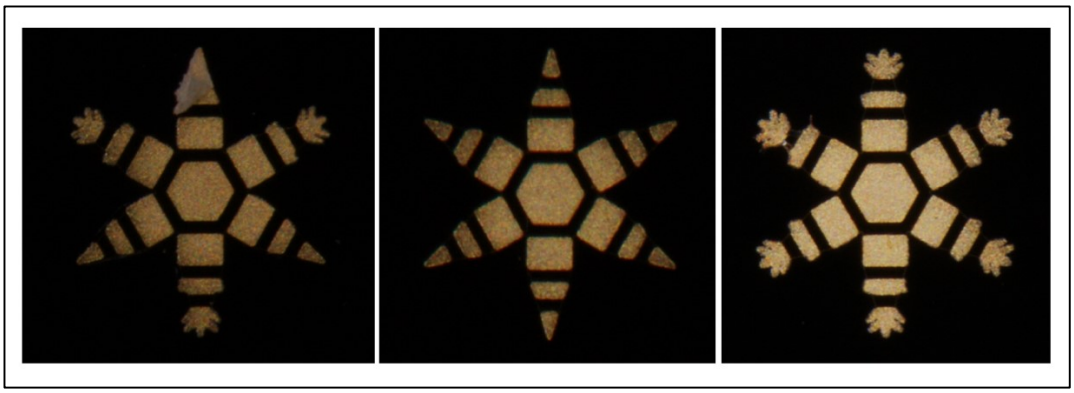

Figure 32: Optical images of different gripper shapes fabricated on 900 um sized (tip-to-tip) grippers. The far left gripper has three arms with with additional small branches. The middle gripper has no additional branches. The far right gripper has additional small branches at the end of each arm.

3.2 Results and Discussion

The overall goal for this study was to use a disease mimicry to randomly apply on the esophagus wall, deploy the microgrippers unbiasedly everywhere on the organ, wait for them to close at body temperature (37°C) and capture tissue, and finally retrieve them using a magnet to extract the tissues collected and quantify the percentage of disease detection [FIGURE 33]. However, for this statistical sampling with microgrippers, we needed to prepare an ex vivo model before applying it on a live animal. In addition, there were other important elements to consider for this model: unbiased deployment of the grippers in the esophagus, controlling the size of diseased area for later calculations, cost and type of the disease model, and the biocompatibility of the grippers. Before going on the live animal biopsy, these parameters needed to be determined.

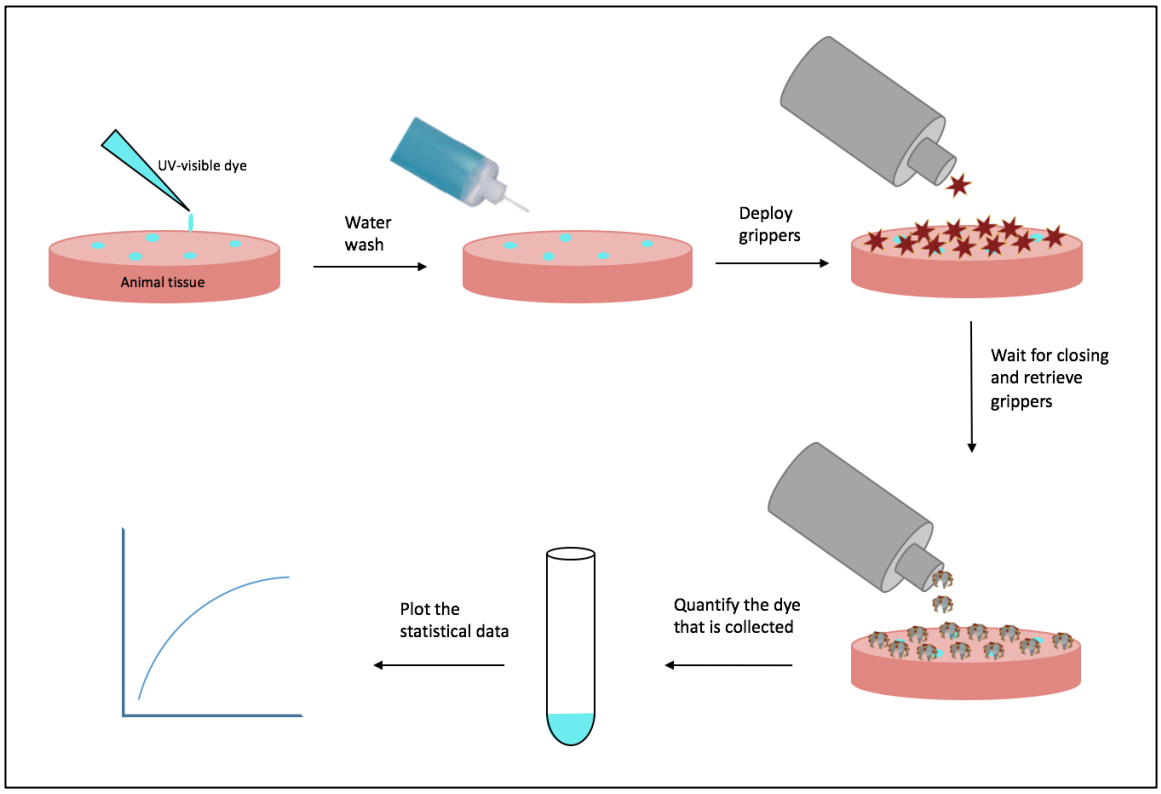

Figure 33: Schematic showing the overall plan for the ex vivo statistical sampling.

The first issue was the blindness to the diseased spot during the deployment of the microgrippers inside the organ to ensure that the results were all unbiased. After searching for cancer disease models, we realized that it wasn't very effective and cheap to actually seed cancer cells or cause mutation which will progress into a disease in the esophagus. In the past, esophagus tattooing has been abundantly used for esophageal biopsies because of their adhesion to the mucosa layer on top of the epithelial cells.[53,54,55] However, these dyes are visible under the normal light and would not provide an unbiased spreading of the grippers inside the esophagus because they can be seen with the endoscope camera. Therefore, we investigated a commercial UV-visible skin marking ink, Sirchie ©, that is designed to stain and stay on the skin. The dye was made up of 93.8% ethanol, 5% water, and 1.2% disodium 4,4'-bis[[4-anilino-6-[(2-

carbamoylethyl)(2- hydroxyethyl)amino]-1,3,5,-triazin-2-yl]amino]stilbene-2,2'-disulphonate, which is the fluorescent dye molecule in the mixture. It looked clear under the visible light, and when excited with UV light (350-360 nm), it emitted a blue color [FIGURE 34]. This dye was cheaper and easier to use compared to the other disease models for our purposes.

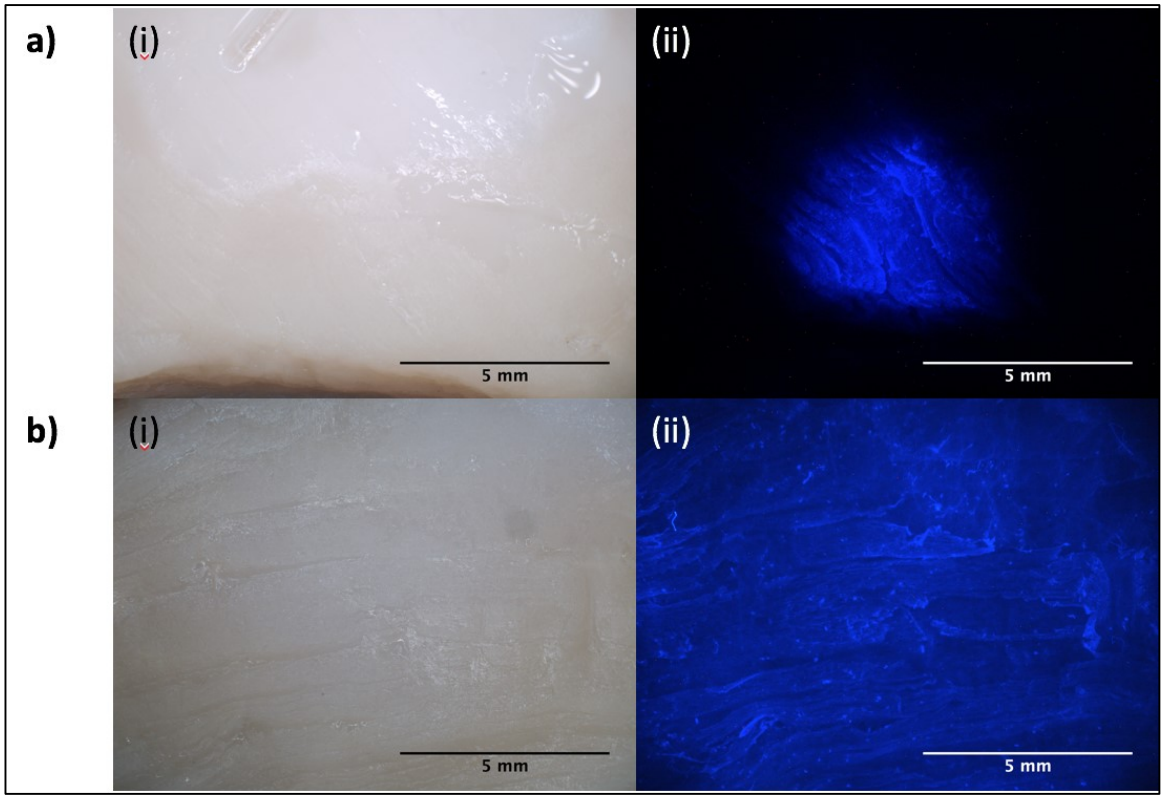

Figure 34: Fluorescent images of the Sirchie© dye. A) (i) Bright-field image of a dyed spot and (ii) fluorescent image of (i) with the dyed spot seen in blue color. B) (i) Bright-field image of a completely dyed tissue and (ii) fluorescent image of (ii) with the blue color showing everywhere.

To test the dye, we first cleaned pieces of chicken breast that were purchased from a supermarket and applied different number of UV dye spots on each piece using a simple pneumatic pump attached to a catheter with a wetted cotton tip at the end. Before using this system, we created a correlation curve between the flow rate and the size of the

dye spot [FIGURE 35]. The smallest dye spot we achieved with this device was 5 mm in diameter, which corresponded to an area of 0.196 cm^2. Assuming the average surface area of an esophagus to be 235 cm^2, we could show the resolution of microgrippers by detecting as small as 0.0835% of the whole esophagus area.[56] In the calibration curve, the deviation in the mean size increased as the dye size increased because the dye flowed into the crevices of the tissue instead of staying in a dot shape. However, this is not a problem for our future steps because instead of applying large dye spots, we can apply frequent smaller dye spots for the statistical sampling. It is important to note that this data was a preliminary result, but it provided an initial control over the spot size for our ex vivo studies. After rinsing the pieces with DI water to mimic the aqueous environment inside the esophagus, we incubated the chicken pieces at 37°C for 30 minutes. Later, we spread the grippers everywhere on top of the tissue in a water based medium using a transfer pipette and incubate the tissues for another hour at 37°C to facilitate the folding of the gripper arms. Finally, we collected the grippers using a small magnet and imaged the collected tissues using fluorescent microscopy [FIGURE 36]. The aim for this experiment was to test our dye with gripper capture, hence we did not do a percentage calculation of dyed-tissue captured grippers and no capture grippers.

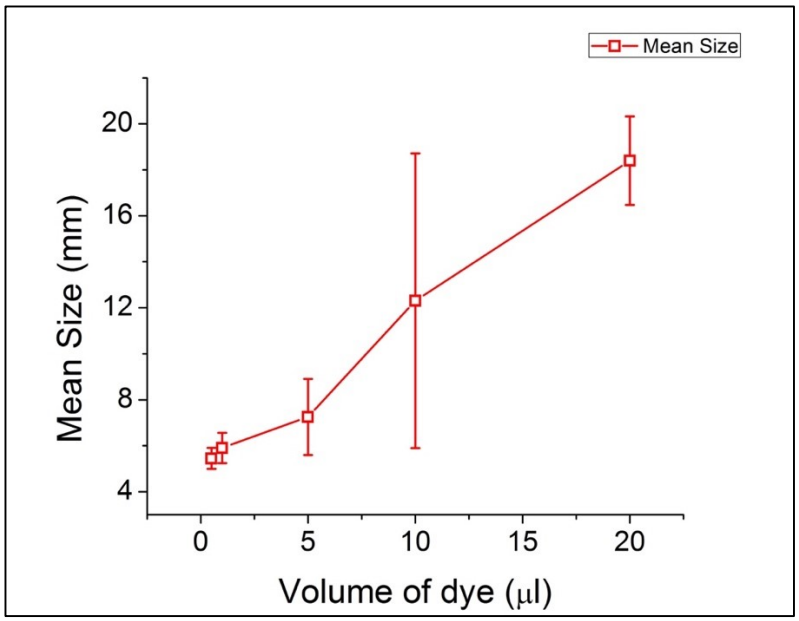

Figure 35: Preliminary correlation graph between the pneumatic pump flow rate and the size of the dye spot.

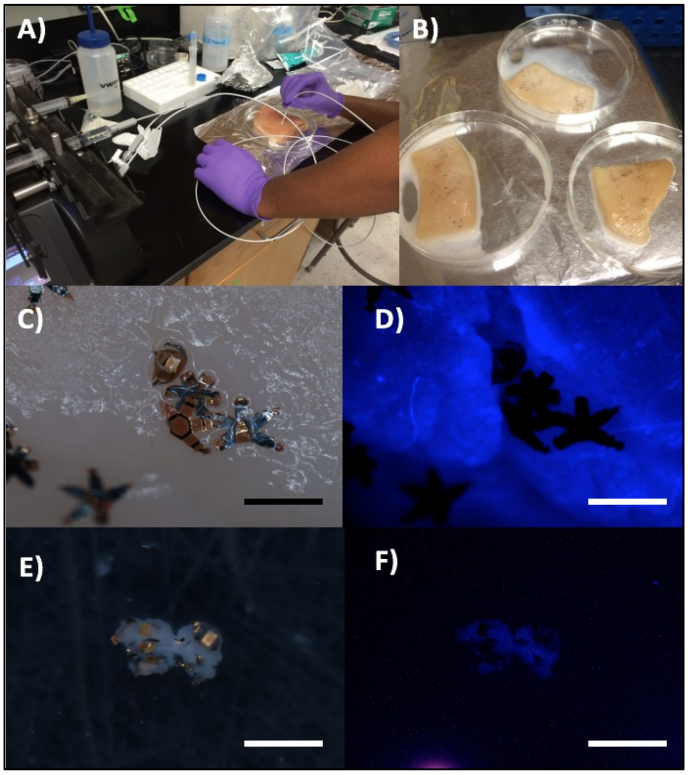

Figure 36: Initial sampling experiments. A) Application of dye spots on the tissue. B) Deployed grippers on the tissue before incubation. C) Bright-field image of the grippers closing on the tissue before retrieval. D) Fluorescent image of (C). The blue color indicates the dyed tissue. E) Bright-filed image of the grippers after retrieval. F) Fluorescent image of (E). The blue color indicates the dyed tissue. (Scale bar in (c-f) is 1 mm).

In parallel to the experimental design improvements, we also investigated different trigger layers for these grippers. In a previously published paper from our lab, a photoresist mix (S1813 and S1805 mixed in a 1:5 ratio) was used as the trigger layer, which was not a biocompatible material.[52,24] Hence, we investigated a biocompatible polymer, called paraffin wax, which is a mixture of long-chain hydrocarbon molecules with a melting temperature of approximately 37°C and a volume expansion of 10-15% from its solid to liquid phase. Paraffin's convenient mechanical and electrical properties (i.e. being an excellent insulator) became very useful as thermal microactuators in the microelectromechanical systems (MEMS) field.[57] Therefore, we purchased a bulk paraffin wax in solid phase from Sigma Aldrich and applied it on the 900 μm size microgrippers using a spin coater and a heat gun to ensure the liquid state of paraffin during spinning.

At the last step of the fabrication for the 900 μm grippers, we varied the spin coating speeds to evenly spread a thick layer of molten paraffin on the grippers. We coated them with spin speeds of 500, 1000, 1500 and 2000 rpm. We also examined the refrigeration effects at 4°C after spin coating at 500 rpm and 1500 rpm to improve the adhesion. The qualifications for the coverage was to have a gripper fully covered with paraffin. Even if one arm was not covered, we didn't consider it as a full coverage [FIGURE 37].

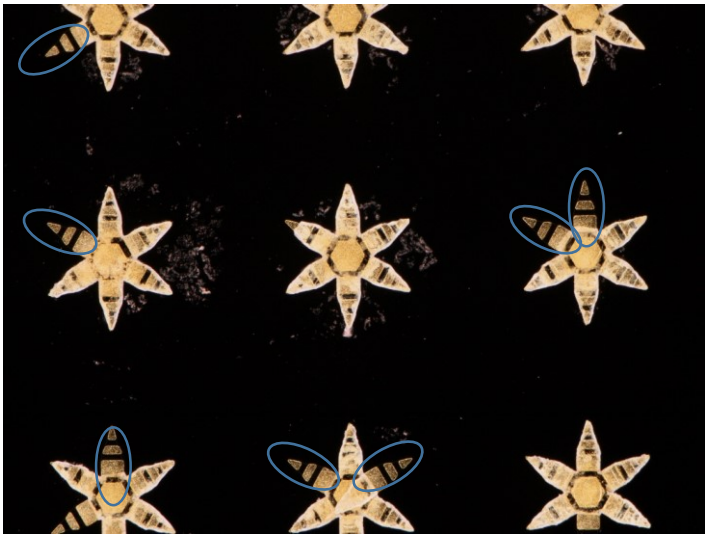

Figure 37: Bright-field image of paraffin covered 900 µm size microgrippers. The blue circles indicate the arms without any paraffin coverage.

We observed that the coverage was better at increased spin speeds, and refrigeration after coating helped the adhesion between paraffin and grippers, most likely due to the rapid hardening of the wax before the grippers were soaked in acetone to lift off the patterned photoresist underneath [FIGURE 38]. Immediately after the coating, we lifted off the grippers form the wafer and submerged them in DI water. We heated up the water to 40°C to let the paraffin expand and fold the arms. However, the paraffin wax is a hydrophobic polymer in nature. Since we coated the paraffin everywhere, the grippers also became hydrophobic and floated on the surface instead of falling into the water [FIGURE 39].

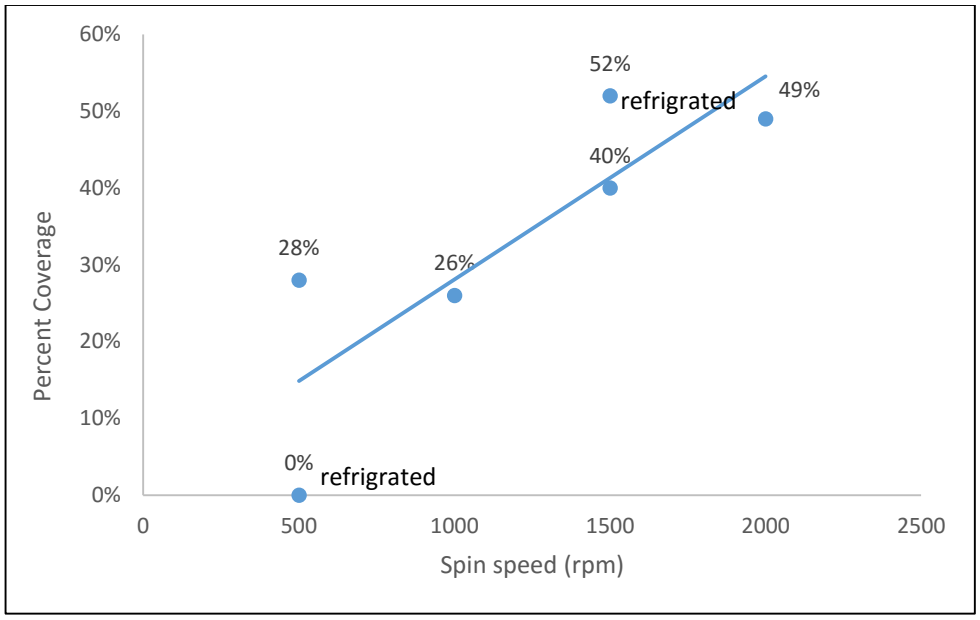

Figure 38: Graph depicting the effect of spin speed on the paraffin coverage on the grippers.

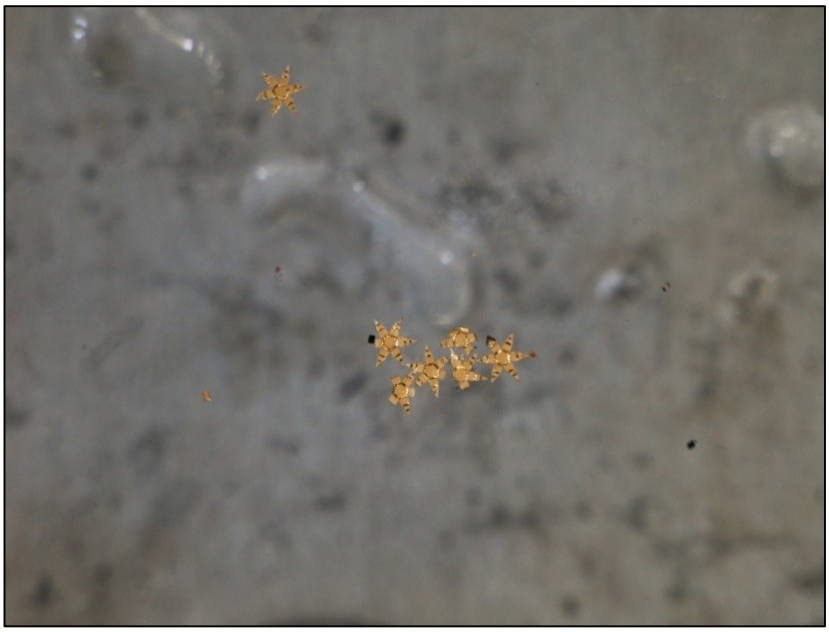

Figure 39: Bright-field image of the paraffin coated grippers floating on the water surface due to the hydrophobic forces that paraffin exerts at the gripper-water interface.

Finally, we tried a different trigger layer using pluronic F-127 gel. Pluronic F-127 is a triblock polymer made up of poly(ethylene oxide) blocks and poly(propylene oxide) blocks. This gel is mainly used in industry as detergents, stabilizers, foaming agents, and emulsifiers. At low temperatures, it has only weak hydrophobic properties, and when the temperature is increased, it becomes hydrophilic.[58] We tried two spin coating speeds to investigate the coverage and mechanical properties of this gel as the trigger layer. Since its viscosity was high, we had to use high spin speeds at 3000 rpm and 4000 rpm in order to spread it on the grippers. Although we used very high spin speeds, pluronic gel was not uniformly covering the grippers. In addition, the lift off process for the photoresist underneath took a very long time (>1 hour), and thus we weren't able to pattern the gel only on the grippers [FIGURE 40]. We concluded that this gel was not a convenient material to use but it can be modified by mixing in different ratios of block polymers to change the viscosity of the gel.

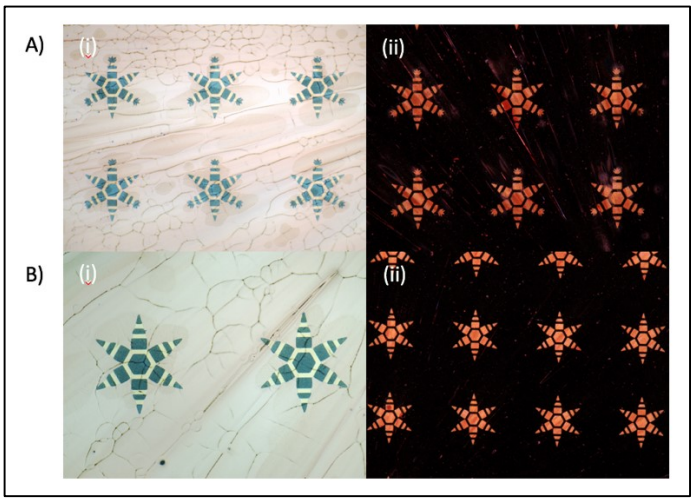

Figure 40: Bright-field images of pluronic F-127 gel as the trigger layer A) with 3000 rpm spin speed (i) before lifting off the photoresist and (ii) after the lift off process, B) with 4000 rpm spin speed (i) before the lift off (ii) after the lift off. (The gripper size is 900 µm tip-to-tip.)

3.3 Conclusion and future work

In summary, the goal of this project was to improve upon the well-established thermally-responsive microgrippers created previously in our lab. To be able to carry these devices in to the field of medicine, especially in pre-cancerous lesion diagnostics, we first needed to show the resolution advantage of them over the traditional forceps in a live animal esophageal biopsy. Before going into surgery with a live animal, we tested our disease model using a UV-visible skin marking ink on chicken breast with microgrippers having the photoresist mixture as the trigger layer. However, due to the toxicity of the photoresists, we modified the trigger layer with paraffin wax that can soften above 37°C and facilitate folding of the arms. We were able to evenly coat the grippers with paraffin. Although this was the goal, we observed that when the grippers were in water, they floated on the surface instead of dipping into the water. We concluded that this was because of the highly hydrophobic nature of the paraffin polymer. This could be a problem in our design because we deploy the microgrippers on to a tissue in cold water. In addition, the esophagus wall is covered with mucosa, which is mostly water. If the grippers repel water, we won't be able retrieve any tissue. As our next step, we planned to design a lithography photomask that will allow us to photopattern the flexible hinges so we can coat paraffin only on the hinges. The paraffin trigger layer only has to naturalize the force exerted on the bilayer, which is on the flexible hinges, hence we can decrease the surface area of the paraffin on the gripper and thus make the gripper less hydrophobic. In addition, we can functionalize the Au panels with a thiol (i.e. 11-mercapto-1-undecanol) that has a hydrophilic terminal group [FIGURE 41]. This way we can increase the hydrophilicity of the grippers.

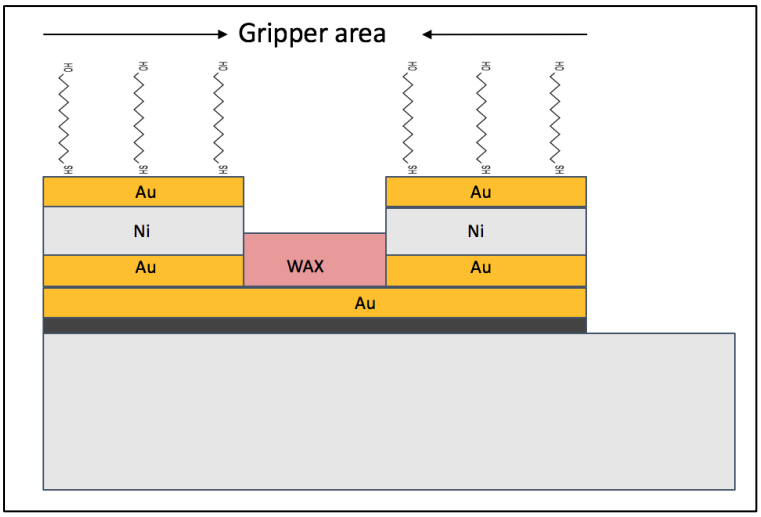

Figure 41: Schematic describing the future work of patterning the paraffin only on the hinges and functionalizing the Au panels with a hydrophilic thiol.

Finally, we plan to incorporate mucin gel with our UV-visible dye to apply on the esophagus wall for disease model, because we faced some issues when we tried to stain the chicken breast while it was submerged in water [FIGURE 42]. Since the dye solution was in 93.8% ethanol, it immediately dissolved into the water when we pumped it through the catheter and didn't stain the chicken breast. As our future work, we plan to mix the dye with mucin gel and apply the gel as our disease model. Since the top layer of the esophagus wall is covered with mucosa, the gel should adhere well enough and stay in place rather than getting washed away.

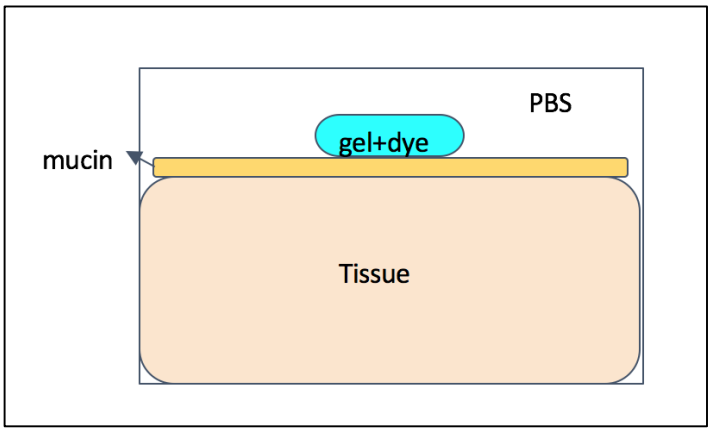

Figure 42: Schematic showing the future work for the UV-visible dye application in the tissue surface in an aqueous environment.

Chapter 4: Conclusion

In this thesis, I aimed to provide a review of different microgripper designs since the beginning of this technology and introduce our microgripper design as a competitor. Firstly, our microgripper design has the advantage of being tetherless for increased maneuverability in 2D and 3D planes. Secondly, they have a pre-stressed self-actuating mechanism built in the arms, which eliminates the need for external power source. Thirdly, they are made up of biocompatible materials, which makes them suitable for in vivo and in vitro applications. Last but not least, they have flexible design aspects for incorporating any new material or hierarchical structure on the grippers. Depending in their size, they can be used for in vitro and in vivo single cell capture or in vivo surgical operations on the sub-millimeter tissue level.

On the single cell level, we designed microgrippers that were made up of biocompatible and transparent materials (SiO and SiO_2) and captured different types of mammalian cells (mouse fibroblast and RBC) in vitro. Moreover, we demonstrated multiple assays on the captured cells, such as a fluorescent cell viability test (calcein AM) and surface-enhanced Raman spectroscopy to detect cell membrane lipids and nucleic acids in the cells. SERS analysis allowed us to do 3D molecule profiling as well as dynamic degradation analysis on 4- NTP molecule attached to AuNS on glass beads. Both assays were successful, such that the results from the fibroblast and red blood cell captures got published, whereas the results for the SERS coupled capture of breast cancer cells is in the process for another publication. Since these grippers are not cell specific, in the future we can modify the surface by attaching antibodies corresponding to the overly expressed cell membrane receptors in cancer cells or in any cell in interest. This way we

can increase the sensitivity and specificity of our grippers making them robust tools for single cell analysis. Moreover, we can add an appropriate actuation mechanism on these grippers, such as enzymatically or thermally triggered polymers, to use them in vivo (i.e. capillary veins, central nervous system, urinary tract, and other tight, hard-to-reach places in body). To be able to control the motion in vivo, we would implement ferromagnetic materials (e.g. Ni) and guide them to the desired spots using magnetic fields or magnets.

For the surgical grippers, we designed a resolution study in the esophagus (a large area organ) to fill in the need for a statistical sampling data in a live animal model using the modified biocompatible grippers. We modeled the diseased areas with a UV-sensitive dye so that the spreading of the grippers in the organ is done as unbiasedly as possible for trustworthy results. Before the biopsy on a live animal model, we tested the dye on chicken breasts and characterized the pneumatic pump in order to get desired spot size on the tissue. We achieved the smallest spot size of 5 mm in diameter with 1 μl/min flow rate, which corresponded to 0.083% of the average human esophagus area. These results were preliminary and open for optimization. Additionally, we contributed to the old design of surgical microgrippers with a relatively new, but less characterized trigger layer, paraffin wax. We achieved a way to coat the molten paraffin on the grippers more uniformly than reported before using spin speeds above 1000 rpm. With the design of a new photomask that patterns only the hinges, we can decrease the hydrophobic behavior of the grippers by reducing the surface area of paraffin on the gripper. As for future work, we can also try to load the paraffin wax (or a hydrogel with similar mechanical properties) with a desired drug and demonstrate drug delivery using the microgrippers. If it works, our grippers can be capable of achieving both diagnosis, and drug delivery at

the same time, which is not a property that any current bioMEM structure has shown in vivo.

In conclusion, I would like to state that I have learned many useful lab techniques and exercises during my years working on these microgrippers. I have mastered designing and fabricating microstructures (e.g. thermal and e-beam thin film evaporation, lithography, electroplating, and O_2 plasma etching). I have also gained a lot of experience in cell culture (maintenance of a culture, and cell counting) and fluorescent imaging (cell viability tests). I have learned and practiced scanning electron microscopy. Finally, working on the microgrippers not only gained me publications but also substantial lab practice and discipline.

References

1. Sun X, Chen W, Tian Y, et al. A novel flexure-based microgripper with double amplification mechanisms for micro/nano manipulation. *Rev Sci Instrum*. 2013;84(8):1-11. doi:10.1063/1.4817695.
2. Kim BS, Park JS, Hun Kang B, Moon C. Fabrication and property analysis of a MEMS micro-gripper for robotic micro-manipulation. *Robot Comput Integr Manuf*. 2012;28(1):50-56. doi:10.1016/j.rcim.2011.06.005.
3. Kim C-J, Pisano AP, Muller RS, Lim MG. Polysilicon microgripper. In: *IEEE 4th Technical Digest on Solid-State Sensor and Actuator Workshop*. IEEE; 1990:48-51. doi:10.1109/SOLSEN.1990.109818.
4. Kim C-J, Pisano AP, Muller RS. Silicon-processed overhanging microgripper. *J Microelectromechanical Syst*. 1992;1(1):31-36. doi:10.1109/84.128053.
5. Wang Z, Shen X, Chen X. Design, modeling, and characterization of a MEMS electrothermal microgripper. *Microsyst Technol*. 2015;21(11):2307-2314. doi:10.1007/s00542-014-2404-4.
6. Pister KSJ, Judy MW, Burgett SR, Fearing RS. Microfabricated hinges. *Sensors Actuators A Phys*. 1992;33(3):249-256. doi:10.1016/0924-4247(92)80172-Y.
7. Lee AP, Ciarlo DR, Krulevitch PA, Lehew S, Trevino J, Northrup MA. A practical microgripper by fine alignment, eutectic bonding and SMA actuation. *Sensors Actuators, A Phys*. 1996;54(1-3):755-759. doi:10.1109/SENSOR.1995.721823.
8. Jager EW, Inganäs O, Lundström I. Microrobots for micrometer-size objects in aqueous media: potential tools for single-cell manipulation. *Science*. 2000;288(5475):2335-2338. doi:10.1126/science.288.5475.2335.
9. Volland BE, Heerlein H, Rangelow IW. Electrostatically driven microgripper. *Microelectron Eng*. 2002;61-62:1015-1023. doi:10.1016/S0167-9317(02)00461-6.
10. Wierzbicki R, Houston K, Heerlein H, et al. Design and fabrication of an electrostatically driven microgripper for blood vessel manipulation. *Microelectron Eng*. 2006;83(4-9 SPEC. ISS.):1651-1654. doi:10.1016/j.mee.2006.01.110.
11. Luo JK, Huang R, He JH, et al. Modelling and fabrication of low operation temperature microcages with a polymer/metal/DLC trilayer structure. *Sensors Actuators, A Phys*. 2006;132(1 SPEC. ISS.):346-353. doi:10.1016/j.sna.2006.03.004.
12. Lu YW, Kim CJ. Microhand for biological applications. *Appl Phys Lett*. 2006;89(16):2004-2007. doi:10.1063/1.2362602.
13. Beyeler F, Neild A, Oberti S, et al. Monolithically fabricated microgripper with integrated force sensor for manipulating microobjects and biological cells aligned in an ultrasonic field. *J Microelectromechanical Syst*. 2007;16(1):7-15. doi:10.1109/JMEMS.2006.885853.
14. Hoxhold B, Büttgenbach S. Easily manageable, electrothermally actuated silicon micro gripper. *Microsyst Technol*. 2010;16(8-9):1609-1617. doi:10.1007/s00542-010-1040-x.
15. Zubir MNM, Shirinzadeh B, Tian Y. Development of a novel flexure-based microgripper for high precision micro-object manipulation. *Sensors Actuators, A Phys*. 2009;150(2):257-266. doi:10.1016/j.sna.2009.01.016.
16. Hsu C, Hsu W. Design and characterization of an electrothermally driven

monolithic long-stretch microdrive in compact arrangement. *J Microelectromechanical Syst*. 2006;15(4):935-944. doi:10.1109/JMEMS.2005.859104.
17. Choi H-S, Lee D-C, Kim S-S, Han C-S. The Development of a Microgripper With a Perturbation-Based Configuration Design Method. *J Micromechanics Microengineering*. 2005;15(6):1327-1333. doi:10.1088/0960-1317/15/6/026.
18. Colinjivadi KS, Lee JB, Draper R. Viable cell handling with high aspect ratio polymer chopstick gripper mounted on a nano precision manipulator. *Microsyst Technol*. 2008;14(9-11):1627-1633. doi:10.1007/s00542-008-0580-9.
19. Roch I, Bidaud P, Collard D, Buchaillot L. Fabrication and characterization of an SU-8 gripper actuated by a shape memory alloy thin film. *J Micromechanics Microengineering*. 2003;13:330-336. doi:10.1088/0960-1317/13/2/323.
20. Seidemann V, Bütefisch S, Büttgenbach S. Fabrication and investigation of in-plane compliant SU8 structures for MEMS and their application to micro valves and micro grippers. *Sensors Actuators, A Phys*. 2002;97-98:457-461. doi:10.1016/S0924-4247(01)00829-9.
21. Zhang R, Chu J, Wang H, Chen Z. A multipurpose electrothermal microgripper for biological micro-manipulation. *Microsyst Technol*. 2013;19(1):89-97. doi:10.1007/s00542-012-1567-0.
22. Leong TG, Randall CL, Benson BR, Bassik N, Stern GM, Gracias DH. Tetherless thermobiochemically actuated microgrippers. *Proc Natl Acad Sci U S A*. 2009;106(3):703-708. doi:10.1073/pnas.0807698106.
23. Bassik N, Brafman A, Zarafshar AM, et al. Enzymatically triggered actuation of miniaturized tools. *J Am Chem Soc*. 2010;132(46):16314-16317. doi:10.1021/ja106218s.
24. Gultepe E, Randhawa JS, Kadam S, et al. Biopsy with thermally-responsive untethered microtools. *Adv Mater*. 2013;25(4):514-519. doi:10.1002/adma.201203348.
25. Gultepe E, Yamanaka S, Laflin KE, et al. Biologic tissue sampling with untethered microgrippers. *Gastroenterology*. 2013;144(4):691-693. doi:10.1053/j.gastro.2013.01.066.
26. Marusyk A, Polyak K. Tumor heterogeneity: causes and consequences. *Biochim Biophys Acta*. 2011;1805(1):1-28. doi:10.1016/j.bbcan.2009.11.002.Tumor.
27. Hoppe PS, Coutu DL, Schroeder T. Single-cell technologies sharpen up mammalian stem cell research. *Nat Cell Biol*. 2014;16(10):919-927. doi:10.1038/ncb3042.
28. Powell AA, Talasaz AH, Zhang H, et al. Single cell profiling of Circulating tumor cells: Transcriptional heterogeneity and diversity from breast cancer cell lines. *PLoS One*. 2012;7(5). doi:10.1371/journal.pone.0033788.
29. Bonner WA, Hulett HR, Sweet RG, Herzenberg LA. Fluorescence activated cell sorting. *Rev Sci Instrum*. 1972;43(3):404-409. doi:10.1063/1.1685647.
30. Mazutis L, Gilbert J, Ung WL, Weitz DA, Griffiths AD, Heyman JA. Single-cell analysis and sorting using droplet-based microfluidics. *Nat Protoc*. 2013;8(5):870-891. doi:10.1038/nprot.2013.046\rhttp://www.nature.com/nprot/journal/v8/n5/abs/nprot.2013.046.html#supplementary-information.

31. Carlo D Di, Aghdam N, Lee LP. Single-Cell Enzyme Concentrations , Kinetics , and Inhibition Analysis Using High-Density Hydrodynamic Cell Isolation Arrays Single-Cell Enzyme Concentrations , Kinetics , and Inhibition Analysis Using High-Density Hydrodynamic Cell Isolation Arrays. *Anal Chem*. 2006;78(14):4925-4930. doi:10.1021/ac060541s.
32. Emmert-buck AMR, Bonner RF, Smith PD, et al. Laser Capture Microdissection Published by : American Association for the Advancement of Science Stable URL : http://www.jstor.org/stable/2891306 Accessed : 03-04-2016 22 : 38 UTC Your use of the JSTOR archive indicates your acceptance of the Terms & Cond. 2016;274(5289):998-1001.
33. Rimstidt JD, Barnes HL. The kinetics of silica-water reactions. *Geochim Cosmochim Acta*. 1980;44(11):1683-1699. doi:10.1016/0016-7037(80)90220-3.
34. Hwang S, Tao H, Kim D, et al. NIH Public Access. 2013;337(6102):1640-1644. doi:10.1126/science.1226325.A.
35. Malachowski K, Jamal M, Jin Q, Polat B, Morris CJ, Gracias DH. Self-folding single cell grippers. *Nano Lett*. 2014;14(7):4164-4170. doi:10.1021/nl500136a.
36. Smith EJ, Xi W, Makarov D, et al. Lab-in-a-tube: ultracompact components for on-chip capture and detection of individual micro-/nanoorganisms. *Lab Chip*. 2012;12:1917. doi:10.1039/c2lc21175k.
37. Perkins EM, McCaffery JM. Conventional and immunoelectron microscopy of mitochondria. *Methods Mol Biol*. 2007;372(410):467-483. doi:10.1007/978-1-59745-365-3_33.
38. Kang B, Austin L a, El-Sayed M a. Observing Molecular Events in Real-Time of Apoptosis Dynamics in Living Cancer Cells using Nuclear Targeted Plasmonically Enhanced Raman Nanoprobes. *ACS Nano*. 2014;(5):4883-4892. doi:10.1021/nn500840x.
39. Hoebe RA, Van Oven CH, Gadella TWJ, Dhonukshe PB, Van Noorden CJF, Manders EMM. Controlled light-exposure microscopy reduces photobleaching and phototoxicity in fluorescence live-cell imaging. *Nat Biotechnol*. 2007;25(2):249-253. doi:10.1038/nbt1278.
40. Femino AM. Visualization of Single RNA Transcripts in Situ. *Science (80-)*. 1998;280(5363):585-590. doi:10.1126/science.280.5363.585.
41. Yu J, Xiao J, Ren X, Lao K, Xie XS. Probing Gene Expression in Live Cells, One Protein Molecule at a Time. *Science (80-)*. 2006;311(5767):1600-1603.
42. Lane LA, Qian X, Nie S. SERS Nanoparticles in Medicine: From Label-Free Detection to Spectroscopic Tagging. *Chem Rev*. 2015;115(19):10489-10529. doi:10.1021/acs.chemrev.5b00265.
43. Brolo A. Plasmonics for future biosensors. *Nat Photonics*. 2012;6(November):709-713. doi:DOI 10.1038/nphoton.2012.266.
44. Halas NJ, Lal S, Chang WS, Link S, Nordlander P. Plasmons in strongly coupled metallic nanostructures. *Chem Rev*. 2011;111(6):3913-3961. doi:10.1021/cr200061k.
45. Moskovits M. Surface-Enhanced Raman Spectroscopy: a Brief Perspective. In: Kneipp K, Kneipp H, eds. *Surface-Enhanced Raman Scattering: Physics and Applications*. Springer Berlin Heidelberg; 2006:1-18.
46. Li M, Kang JW, Dasari RR, Barman I. Shedding light on the extinction-

enhancement duality in gold nanostar-enhanced Raman spectroscopy. *Angew Chemie - Int Ed*. 2014;53(51):14115-14119. doi:10.1002/anie.201409314.
47. Kampen KR. Membrane proteins: the key players of a cancer cell. *J Membr Biol*. 2011;242(2):69-74. doi:10.1007/s00232-011-9381-7.
48. Carter P, Smith L, Ryan M. Identification and validation of cell surface antigens for antibody targeting in oncology. *Endocr Relat Cancer*. 2004;11(4):659-687. doi:10.1677/erc.1.00766.
49. Winawer S, Fletcher R, Rex D, et al. Colorectal cancer screening and surveillance: Clinical guidelines and rationale - Update based on new evidence. *Gastroenterology*. 2003;124(2):544-560. doi:10.1053/gast.2003.50044.
50. Tomizawa Y, Wang KK. Screening, Surveillance and Prevention for the Esophageal Cancer. *Gastroenterol Clin North Am*. 2009;38(1):59-73. doi:10.1016/j.gtc.2009.01.014.
51. Yim S, Gultepe E, Gracias DH, Sitti M. Biopsy using a magnetic capsule endoscope carrying, releasing, and retrieving untethered microgrippers. *IEEE Trans Biomed Eng*. 2014;61(2):513-521. doi:10.1109/TBME.2013.2283369.
52. Pandey S, Gultepe E, Gracias DH. Origami inspired self-assembly of patterned and reconfigurable particles. *J Vis Exp*. 2013;(72):e50022. doi:10.3791/50022.
53. Kethu SR, Banerjee S, Desilets D, et al. Endoscopic tattooing. *Gastrointest Endosc*. 2010;72(4):681-685. doi:10.1016/j.gie.2010.06.020.
54. Pohl J. Endoscopic Tattooing. *Video J Encycl GI Endosc*. 2013;1(2):355-356. doi:10.1016/S2212-0971(13)70155-9.
55. Luigiano C, Ferrara F, Morace C, et al. Endoscopic tattooing of gastrointestinal and pancreatic lesions. *Adv Ther*. 2012;29(10):864-873. doi:10.1007/s12325-012-0056-2.
56. Helander HF, Fändriks L. Surface area of the digestive tract - revisited. *Scand J Gastroenterol*. 2014;49(6):681-689. doi:10.3109/00365521.2014.898326.
57. Ogden S, Klintberg L, Thornell G, Hjort K, Boden R. Review on miniaturized paraffin phase change actuators, valves, and pumps. *Microfluid Nanofluidics*. 2014;17(1):53-71. doi:10.1007/s10404-013-1289-3.
58. Bercea M, Darie RN, Nita LE, Morariu S. Temperature responsive gels based on Pluronic F127 and poly(vinyl alcohol). *Ind Eng Chem Res*. 2011;50(7):4199-4206. doi:10.1021/ie1024408.